NASA CONTRACTOR REPORT

QUASI-OPTIMUM DESIGN OF CONTROL SYSTEMS FOR MOVING-BASE SIMULATORS

by Bernard Friedland and Chong K. Ling

Prepared by
SINGER-GENERAL PRECISION
Little Falls, N. J. 07424
for Ames Research Center

NATIONAL AERONAUTICS AND SPACE ADMINISTRATION • WASHINGTON, D. C. • OCTOBER 1970

1. Report No. NASA CR-1613	2. Government Accession No.	3. Recipient's Catalog No.
4. Title and Subtitle: Quasi-Optimum Design of Control Systems for Moving-Base Simulators		5. Report Date: October 1970 6. Performing Organization Code
7. Author(s): Bernard Friedland and Chong K. Ling		8. Performing Organization Report No.
9. Performing Organization Name and Address: Singer-General Precision, 1150 McBride Avenue, Little Falls, New Jersey 07424		10. Work Unit No. 11. Contract or Grant No. NAS 2-3636 13. Type of Report and Period Covered: Contractor Report
12. Sponsoring Agency Name and Address		14. Sponsoring Agency Code

15. Supplementary Notes

16. Abstract

This report is concerned with the optimal control of a six-degree-of-freedom moving-base simulator, and utilizes the quasi-optimal control method due to Friedland. The problem, in broad terms, is to determine a control law for moving the simulator cab so that its motion will: (1) "best" approximate the desired aircraft response, and (2) not exceed the limited translational capability of the simulator. Due to lack of experimental data, "best" can only be interpreted subjectively at the present time. By use of the method, a variety of quasi-optimal responses, each emphasizing different features thought to be important in motion perception, have been obtained. Examples of such results are given, and the considerations important in initial subjective evaluations by experienced flight personnel are discussed. Final evaluation must be made by actual experiments in a motion simulator.

17. Key Words (Selected by Author(s))	18. Distribution Statement
Motion Simulation Motion Simulators Optimal Control	Unclassified-Unlimited

19. Security Classif. (of this report)	20. Security Classif. (of this page)	21. No. of Pages	22. Price*
Unclassified	Unclassified	89	$3.00

*For sale by the Clearinghouse for Federal Scientific and Technical Information
Springfield, Virginia 22151

PREFACE

In the investigation reported herein, a technique of quasi-optimum control, developed under NASA Contract NAS 2-2648 [1] and further studied under Contract NAS 2-3636 [2] (both with the Ames Research Center) is applied to the problem of controlling the motion of the cab in a moving-base simulator. The objective of the design is to provide the pilot with as realistic motion cues as possible within the confines of the limited motion capabilities of the simulator. In the investigation reported only the longitudinal motion is considered; the method employed, however, would appear to be applicable to the more general six-degree-of-freedom case and further investigation of the method is planned.

The principal contributors to the moving-base simulator study were Dr. Bernard Friedland and Dr. Chong K. Ling. In addition to the study of the motion-simulation problem, other aspects of the quasi-optimum control technique were studied during 1969. The results of these studies, to which Dr. Frederick E. Thau contributed, will be reported elsewhere, as appropriate.

The authors are most grateful for the insights gained in several discussions with Messrs. M.D. White, J.G. Douvillier, R.S. Bray, and other members of the Ames Research Center Flight and Systems Simulation Branch, and for the assistance of Dr. E.C. Stewart, of the Theoretical Guidance and Control Branch, who served as Contract Technical Monitor.

CONTENTS

1. INTRODUCTION

A moving-base simulator is a device in which a pilot manipulates a set of flight controls and the cab in which he is situated moves in a manner which tends to reproduce the sensation of motion which would be experienced in the aircraft with the same control inputs. To achieve a high-fidelity simulation, the simulator control system should be designed to keep the errors between the "aircraft" motion and the cab motion as small as possible.

The major problem of the control system design is the limited motion capability of the cab in translation. For a flight simulation mission in which the aircraft would undergo large excursions, the cab motion will necessarily be different from the aircraft motion and the motion simulation will have to be more or less unrealistic.

Given the fact of limited motion in the cab the basic question underlying the design of control system is: what aspects of motion must be reproduced with high fidelity and what aspects of motion can be sacrificed without excessively degrading the realism of the simulation. It is generally accepted that one of the most important factors governing the realism of a simulation is the kinesthetic sensation of motion. Many experimental studies have been performed to establish the connection between actual motion and the subjective sensation thereof. It is generally believed, for example, that only acceleration and its derivatives (but not its integrals) are significant, that there are thresholds below which the sensation of motion is absent, that there exists an amplitude dependent delay time (latency-time) between motion and perception of sensation of motion, that the sensation of a constant acceleration tends to diminish with time as a result of the "adaptation" phenomenon. Although mathematical models have been proposed which account for some or all of these phenomena with varying degrees of success, their validity has been questioned by researchers in various disciplines.

Whether because the validity of the kinesthetic sensor models are questioned, or for other reasons of practical expedience, it appears that the only method currently used for designing motion simulators is empirical: by one means or another a design is achieved, it is

tested by an experienced pilot, and his experience is used as the basis of an altered design. Sooner or later a control system is obtained which performs in some acceptable manner.

One method which is currently used to maintain the excursion of the cab within the allowable limits of motion employs "acceleration washout". Specifically, the aircraft acceleration is passed through a high-pass filter which attenuates the low-frequency components of the acceleration (which result in large excursions) while permitting the high-frequency components to pass through with negligible attenuation. The cab is then controlled to follow this washed acceleration. This system is shown schematically in Fig. 1-1. The parameters of this high-pass filter (e.g., the cutoff frequency ω and damping factor ξ of Fig. 1-1) are adjusted to maintain the cab excursions within acceptable limits.

One of the shortcomings of this design approach is the difficulty of relating the parameters of the high-pass washout filter to the transient response of the cab. Another possible shortcoming of this approach is that the washout is linear. If the parameters of the system are adjusted to washout aircraft accelerations which result in excessive excursions, it will also washout aircraft accelerations which do not result in excessive accelerations, although there would appear to be no reason for so doing. It would appear preferable to employ a nonlinear control scheme in which, if the pilot commands an excursion which is within the cab motion capability, this motion would be followed exactly. The desired situation is illustrated in Figure 1-2. For a large aircraft excursion (a), exceeding the motion limit, the corresponding cab excursion shown in (b) would be desirable; on the other hand, for a small aircraft excursion (c) within the motion capability of the cab, the cab motion should follow (c).

It is generally believed that the empirical solutions to the problem of limited motion lead to designs which do not fully exploit the available motion capabilities of the system. In other words, the washout methods currently employed produce unacceptable sensations of motion for a number of missions and it is felt that the use of more sophisticated design techniques could lead to an increase in the number of missions for which acceptably realistic motion sensations could be achieved.

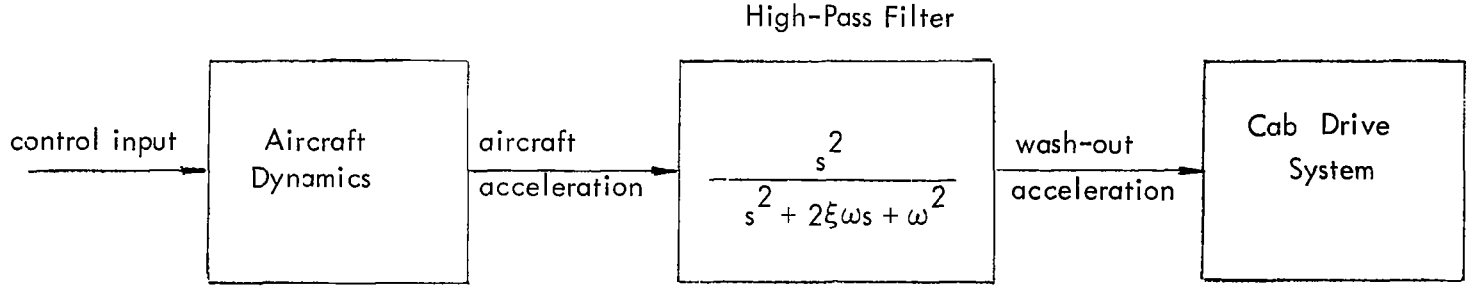

Fig. 1-1

Conventional Wash-Out Block Diagram

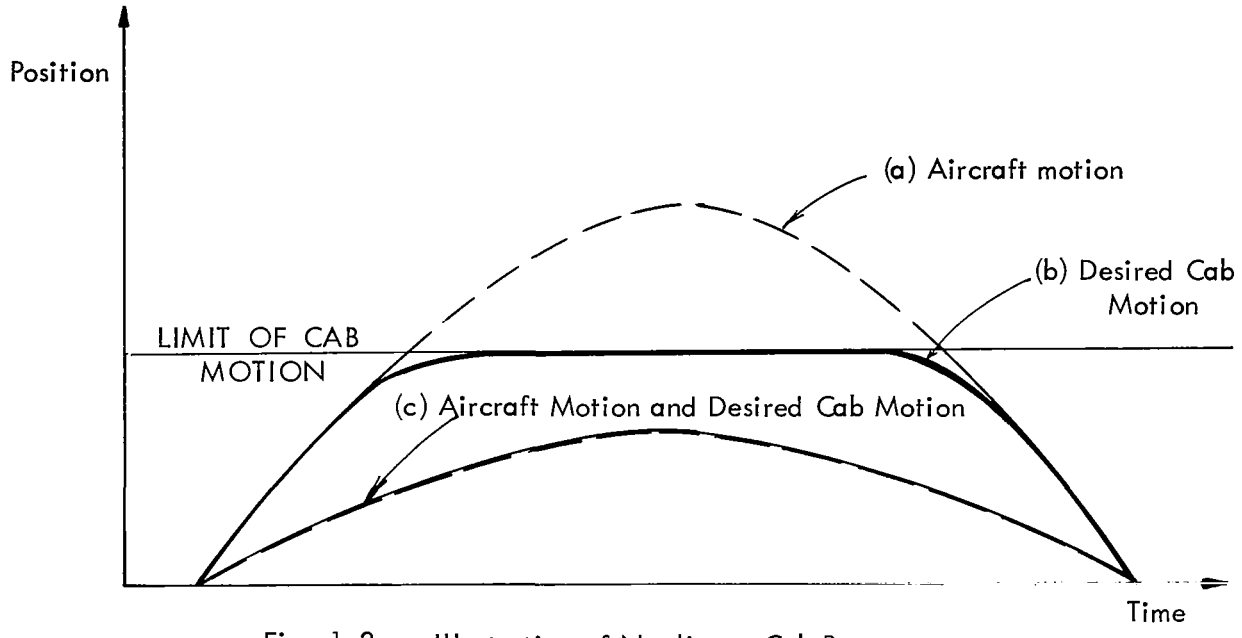

Fig. 1-2 - Illustration of Nonlinear Cab Response

This consideration was the motivation of the study described in this report in which the methodology of optimum control theory was applied to the problem. Attention was confined primarily to the case in which the motion is restricted to 2 degrees-of-freedom, pitch and vertical displacement, such as might represent an aircraft landing under rather idealized circumstances.

The results achieved indicate that the approach studied has considerable merit although it is certainly not without problems, one of the most significant of which is the absence of a completely rational standard of performance evaluation. Thus it would be desirable to continue the investigation to extend the results to the more general case of six degree-of-freedom motion and to endeavor to establish a more rational performance criterion.

This report is organized as follows. The design problem is first formulated in the framework of optimum control theory in Section 2. A general approximate solution to the problem is then derived in Section 3 through the application of the quasi-optimum control

technique. In Section 4 the result of Section 3 is applied to the control of longitudinal motion simulation of a particular aircraft. Finally, the results are discussed and a possible future effort is suggested in Section 5.

2. MATHEMATICAL PROBLEM FORMULATION

2.1 Aircraft and Cab Dynamics

The moving-base simulator of concern in this investigation will be of the type currently in use at the Ames Research Center for which the cab motion is produced by a drive system in which each degree-of-freedom of the cab can be independently controlled. To any degree of accuracy desired, the "aircraft" is represented by a computer with the input proportional to the pilot's command signal and the output representing the aircraft motion. It is assumed that the state variables of the aircraft, which are modeled by the computer, are available for the control of the cab motion. Although it will be ultimately desirable to treat a six degree-of-freedom situation, the present study is confined to a two degree-of-freedom situation in which only pitch and vertical displacement are considered.

The linearized aircraft dynamics can be expressed as

$$\dot{x}_a = A_a x_a + B_a \delta_a \tag{2.1}$$

where x_a is the state vector of an aircraft with components $\{x_{a1}, x_{a2}, \cdots\}$ representing position, velocity, acceleration, pitch, pitch rate, etc., and δ_a is the control surface deflection or its derivative depending on the situation. A_a and B_a are matrices of appropriate dimensions representing the aircraft parameters associated with the state variables x_a and input δ_a, respectively.

Similarly, the corresponding cab dynamics are expressed as

$$\dot{x}_c = A_c x_c + B_c u \tag{2.2}$$

where u is the control input to be generated by the control system to be designed and x_c, A_c and B_c are the cab state vector and the parameter matrices corresponding to x_a, A_a and B_a, respectively.

The difference between the aircraft state and the cab state is denoted by

$$x = x_a - x_c \tag{2.3}$$

and satisfies the differential equation

$$\dot{x} = \dot{x}_a - \dot{x}_c = A_a x_a + B_a \delta_a - A_c x_c - B_c u$$

or

$$\dot{x} = A_a x + (A_a - A_c) x_c + B_a \delta_a - B_c u \tag{2.4}$$

This equation, together with (2.2) comprise the dynamic process for which the control law is to be devised.

In particular, the longitudinal and pitch motion of a typical aircraft governed by the following dynamic equations will be considered:

$$\begin{aligned} \ddot{y}_a + a_a \dot{y}_a - b_a \theta_a &= c_a \delta_a \\ \ddot{\theta}_a + f_a \dot{\theta}_a + e_a \theta_a - d_a y_a &= -g_a \delta_a \end{aligned} \tag{2.5}$$

where y_a is the vertical displacement of the aircraft C. G. relative to earth, θ_a is the pitch angle, and a_a, b_a, c_a, d_a, e_a, f_a, g_a are assumed to be constant coefficients related to the aircraft aerodynamic parameters.

In the event that the motion of a point not at the aircraft C. G. is to be simulated, the dynamics are similar in form to (2.5) except that the vertical acceleration $\ddot{y}_a$ contains a term proportional to $\dot{\theta}_a$ and the constant coefficients are dependent on the moment arm ℓ from the C. G. to the point of interest.

Assuming that each degree-of-freedom of the cab motion is separately governed by a linear second-order driving system, the corresponding cab dynamics can be approximated by

$$\begin{aligned} \ddot{y}_c + 2\xi_1 \omega_1 \dot{y}_c + \omega_1^2 y_c &= u_1 \\ \ddot{\theta}_c + 2\xi_2 \omega_2 \dot{\theta}_c + \omega_2^2 \theta_c &= u_2 \end{aligned} \tag{2.6}$$

where y_c, θ_c are the displacement and the pitch corresponding to y_a, θ_a respectively, u_1 and u_2 are the command signals to each respective driving system, and ξ_1, ω_1, ξ_2, ω_2 are constant parameters.

It is noted that the dynamic equations (2.5) and (2.6) can always be rewritten in the state form of (2.1) and (2.2) by properly defining the state variables as will be seen in the sequel.

2.2 Performance Criteria

It is noted that the primary objective of the control system is to provide, in accordance with the pilot's input, command signals to the simulator drive motors in such a way that the kinesthetic sensation of motion of the pilot situated in the cab is a faithful replica of what he would sense if he were flying the real aircraft. This problem is complicated by the fact that the relation between "how the pilot senses" and "how the cab (or aircraft) moves" is nonlinear in nature due to the existence of "threshold" and "latency time" phenomenon in the human sensory organ. The threshold is known to be the minimum amount of acceleration (or jerk) that can be sensed by a pilot, while the latency time is the minimum amount of (delay) time necessary for a pilot to sense the motion after the vehicle has actually "moved" beyond the threshold. The latency-time is inversely proportional to the magnitude of acceleration (or jerk), and follows an approximately exponential relation. Thus, for a realistic design of the control system, a design criterion (performance index) should be defined to measure the error in perception of motion rather than the motion itself.

It has been well established that the human perception of motion is due to the activation of "vestibular" system within the human body. The vestibular system serves as the principal motion sensing center in the human. The "input" to this human sensory system is the external force acting upon the head and the "output" is the subjective perception of "motion". Therefore, the subjective perception of motion cues by a pilot can be interpreted in terms of the quantitative state of the kinesthetic sensory system provided the dynamics governing the input-output relation of the sensory system are known.

It would ultimately be desirable to utilize the analytical input-output relation of the vestibular system as an aid to the control system design. For the present study, however, an ad-hoc performance criterion was selected based on the following considerations.

Physiological experiments have indicated that the principal kinesthetic cues are primarily those of translational acceleration and its rates and the angular velocity and acceleration. Thus, the simulation will be regarded as realistic if the differences of those quantities between the aircraft and that of the cab are kept to a minimum while maintaining the cab excursion within certain prespecified limits.

Thus, for this purpose, we established the following performance criterion

$$V = \int_{t}^{T+t} M(\ddot{e}_y, \dddot{e}_y, \dot{e}_\theta, \ddot{e}_\theta)\, ds + \epsilon \int_{t}^{T+t} L(y_c)\, ds \tag{2.7}$$

where t is the present time and T is the control interval, e_y and e_θ are the differences between the position and the pitch angle, respectively, of the simulator and that of the aircraft, M is a quadratic form in the error rate and its derivatives, and $L(y_c)$ is a penalty which is imposed for large excursions y_c of the simulator cab from the neutral position. With the penalty multiplier ϵ reduced to zero, the motion of the aircraft and simulator can be made identical, and hence the cab will generally exceed the motion limits. By proper selection of ϵ and $L(y_c)$ it was felt that a suitable compromise between low error rates and derivatives thereof (acceleration, jerk, etc.) and limited motion could be achieved by minimizing V.

In particular, the following forms of M and L functions were used in this investigation:

Linear acceleration weighting:

$$M_1 = \frac{1}{2}(q_{\ddot{y}}\ddot{e}_y^2 + q_{\dot{\theta}}\dot{e}_\theta^2 + q_{\ddot{\theta}}\ddot{e}_\theta^2) \tag{2.8}$$

Linear acceleration and jerk weighting:

$$M_2 = \frac{1}{2}(q_{\ddot{y}}\ddot{e}_y^2 + q_{\dddot{y}}\dddot{e}_y^2 + q_{\dot{\theta}}\dot{e}_\theta^2 + q_{\ddot{\theta}}\ddot{e}_\theta^2) \tag{2.9}$$

and

"Hard" limiting:

$$L_1 = \begin{cases} 0 & |y_c| < Y_c \\ |y_c - Y_c| & |y_c| \geq Y_c \end{cases} \tag{2.10}$$

"Soft" limiting:

$$L_2 = \left(\frac{y_c}{Y_c}\right)^{2\beta} \qquad \beta \geq 1 \tag{2.11}$$

where $q_{\ddot{y}}$, $q_{\dddot{y}}$, $q_{\dot{\theta}}$, $q_{\ddot{\theta}}$ are constant weighting factors, and Y_c is a constant representing the physical boundary for cab excursion. The penalty functions L_1 and L_2 are illustrated in Fig. 2-1.

To facilitate subsequent calculations, the performance integral (2.7) can be rewritten in terms of state variables as

$$V = \frac{1}{2}\int_t^{T+t} (\dot{x}' Q \dot{x})\, ds + \epsilon \int_t^{T+t} L(x_c)\, ds \tag{2.12}$$

where Q is a positive semi-definite matrix with elements $q_{\dot{y}}$, $q_{\dddot{y}}$, $q_{\dot{\theta}}$, $q_{\ddot{\theta}}$ etc.

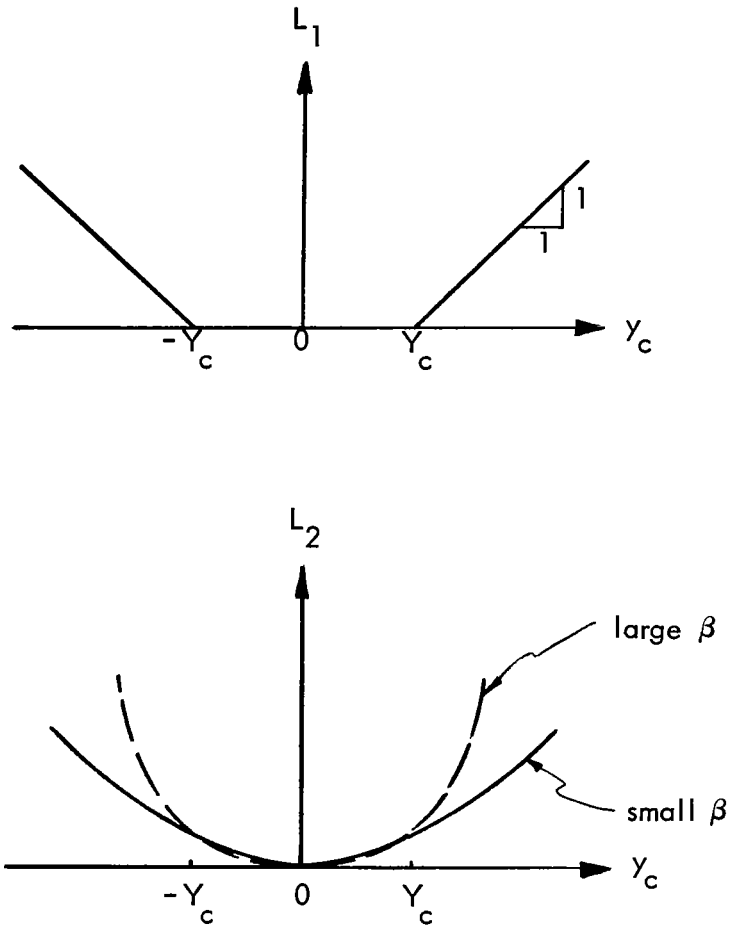

Fig. 2-1

The Penalty Functions

3. APPLICATION OF QUASI-OPTIMUM CONTROL TECHNIQUE

The control problem to be treated consists of the aircraft dynamics (2.1), the cab dynamics (2.2), the "error" dynamics (2.4) and the performance index (2.12), as re-written below.

$$\dot{x}_a = A_a x_a + B_a \delta_a \tag{3.1}$$

$$\dot{x}_c = A_c x_c + B_c u \tag{3.2}$$

Let $x = x_a - x_c$

then $$\dot{x} = A_a x + (A_a - A_c) x_c + B_a \delta_a - B_c u \tag{3.3}$$

$$V = \int_t^{T+t} \left[\frac{1}{2} (\dot{x}' Q \dot{x}) + \epsilon L(x_c)\right] d\tau \tag{3.4}$$

the initial time is taken as the present time t at which the state of the aircraft and cab are given by

$$x_a(t), \quad x_c(t) \tag{3.5}$$

respectively. At the end of the control interval, it is assumed that

$$x_a(T+t), \quad x_c(T+t), \quad x(T+t), \qquad \text{are free} \tag{3.6}$$

and the control u is not explicitly constrained.

It is noted that the error rate $\dot{x}$ in the performance index (3.4) contains velocity, acceleration and possibly higher derivative components. Hence a completely realistic ("one-to-one") simulation is obtained if it is possible to keep $\dot{x} \equiv 0$ with

$$B_c u = A_a x + (A_a - A_c) x_c + B_a \delta_a \tag{3.7}$$

Assuming that (3.7) can be solved for u, the control law obtained is

$$u = K [A_a x + (A_a - A_c) x_c + B_a \delta_a] \tag{3.8}$$

and, from (3.2) and (3.7)

$$\dot{x}_c = A_a x_c + A_a x + B_a \delta_a \tag{3.9}$$

with $\dot{x} \equiv 0$, or $x = \text{const.}$

Also, with $\epsilon = 0$, the performance index (3.4) becomes

$$V = \int_{t}^{T+t} \frac{1}{2} (\dot{x}' Q \dot{x})\, d\tau \tag{3.10}$$

which, together with (3 2) and (3.3), will result in linear control law. Moreover, since $V \equiv 0$ is the absolute minimum of (3.10), and is achieved by (3.7) it is clear that the optimum control law for $\epsilon = 0$ reduces to (3.8).

3.1 Application of Optimal Control Theory

To treat the problem with the dynamic process (3.2) and (3.3) and the performance criterion (3.4), define the adjoint vector

$$p = \begin{bmatrix} p_0 \\ p_c \\ p \\ p_\epsilon \\ p_\tau \end{bmatrix} \tag{3.11}$$

where

p_0 corresponds to the performance

p_c corresponds to the cab state

p corresponds to the error state

p_ϵ corresponds to the multiplier ϵ = const.

p_τ corresponds to time

The Hamiltonian is thus

$$\begin{aligned} h = {} & p_0 \left[\frac{1}{2} (\dot{x}' Q \dot{x}) + \epsilon L(x_c) \right] + p_c' \left[A_c x_c + B_c u \right] \\ & + p' \left[A_a x + (A_a - A_c) x_c + B_a \delta_a - B_c u \right] + p_\tau \end{aligned} \tag{3.12}$$

The corresponding adjoint equations, for $t \le \tau \le T+t$, are

$$\dot{p}_0 = -\frac{\partial h}{\partial x_0} = 0 \tag{3.13}$$

$$\dot{p}_c = -\frac{\partial h}{\partial x_c} = -p_0\{\frac{1}{2}\frac{\partial}{\partial x_c}[\dot{x}'Q\dot{x}] + \epsilon\frac{\partial L}{\partial x_c}\} - A_c'p_c - (A_a - A_c)'p \tag{3.14}$$

$$\dot{p} = -\frac{\partial h}{\partial x} = -p_0\{\frac{1}{2}\frac{\partial}{\partial x}[\dot{x}'Q\dot{x}]\} - A_a'p \tag{3.15}$$

$$\dot{p}_\epsilon = -\frac{\partial h}{\partial \epsilon} = -p_0 L(x_c) \tag{3.16}$$

$$\dot{p}_\tau = -\frac{\partial h}{\partial \tau} \tag{3.17}$$

From (3.13) $p_0 \equiv -1$. Also

$$\frac{1}{2}\frac{\partial}{\partial x_c}(\dot{x}'Q\dot{x}) = (A_a - A_c)'Q[A_a x + (A_a - A_c)x_c + B_a\delta_a - B_c u]$$

$$\frac{1}{2}\frac{\partial}{\partial x}(\dot{x}'Q\dot{x}) = A_a'Q[A_a x + (A_a - A_c)x_c + B_a\delta_a - B_c u]$$

whence (3.14) - (3.16) become

$$\dot{p}_c = (A_a - A_c)'Q[A_a x + (A_a - A_c)x_c + B_a\delta_a - B_c u] + \epsilon\frac{\partial L}{\partial x_c} - A_c'p_c - (A_a - A_c)'p \tag{3.18}$$

$$\dot{p} = A_a'Q[A_a x + (A_a - A_c)x_c + B_a\delta_a - B_c u] - A_a'p \tag{3.19}$$

$$\dot{p}_\epsilon = L(x_c) \tag{3.20}$$

It is assumed that there are no constraints on the control variable u. In this case the maximum principle gives the control law $\partial H/\partial u = 0$, or, from (3.12),

$$\frac{1}{2}\frac{\partial}{\partial u}(\dot{x}' Q\dot{x}) + \frac{1}{p_0} B_c' (p_c - p) = 0 \qquad (3\ 21)$$

or

$$B_c' Q[A_a x + (A_a - A_c) x_c + B_a \delta_a - B_c u] = \frac{1}{p_0} B_c' (p_c - p) \qquad (3.22)$$

Comparing this equation with (3.7) it is observed that (3.7) satisfies (3.22) when when $(p_c - p) \equiv 0$. More generally, if $B_c' Q B_c$ is non-singular, the optimum control law is given by

$$u = (B_c' Q B_c)^{-1} B_c' \{Q[A_a x + (A_a - A_c) x_c + B_a \delta_a] - \frac{(p_c - p)}{p_0}\} \qquad (3.23)$$

The control system based on this equation is shown in Fig. 3-1.

Consider the differential equation for $p_c - p$; from (3.18) and (3.19)

$$\dot{p}_c - \dot{p} = -A_c' (p_c - p) - A_c' Q[A_a x - (A_a - A_c) x_c + B_a \delta_a - B_c u] + \epsilon \frac{\partial L}{\partial x_c} \qquad (3.24)$$

Suppose $\epsilon = 0$, and (3.7) is satisfied. Then (3.24) becomes

$$\dot{p}_c - \dot{p} = -A_c' (p_c - p) \qquad (3.25)$$

which is a homogeneous equation. Moreover, $p_c(T + t) = p(T + t) = 0$ if the terminal state is not specified. Hence, from (3.25) $p_c - p \equiv 0$. Thus it is evident that the control u which satisfies (3.7) satisfies the necessary condition for an optimum control. If $\epsilon \neq 0$, however, then (3.24) is not homogeneous and (3.23) does not result in an optimum control law, since $p_c - p \not\equiv 0$, in general. Since $p_c - p$ increases with the weighting factor ϵ multiplying the penalty $L(x_c)$, the contribution to u due to $p_c - p$ may be attributed in part to the desire to keep x_c within the limits of cab motion. Consequently, the part of feedback quantity $p_c - p$ can be regarded as the "washout" input designed to prevent motion from exceeding the motion limits.

The calculation of this feedback term is the main objective of this analysis. For this purpose it will be necessary to have the complete set of canonical equations, which are obtained by substitution of the optimum control law (3.23) into (3.2), (3.3), (3.18) and (3.19). The results can be arranged in matrix form

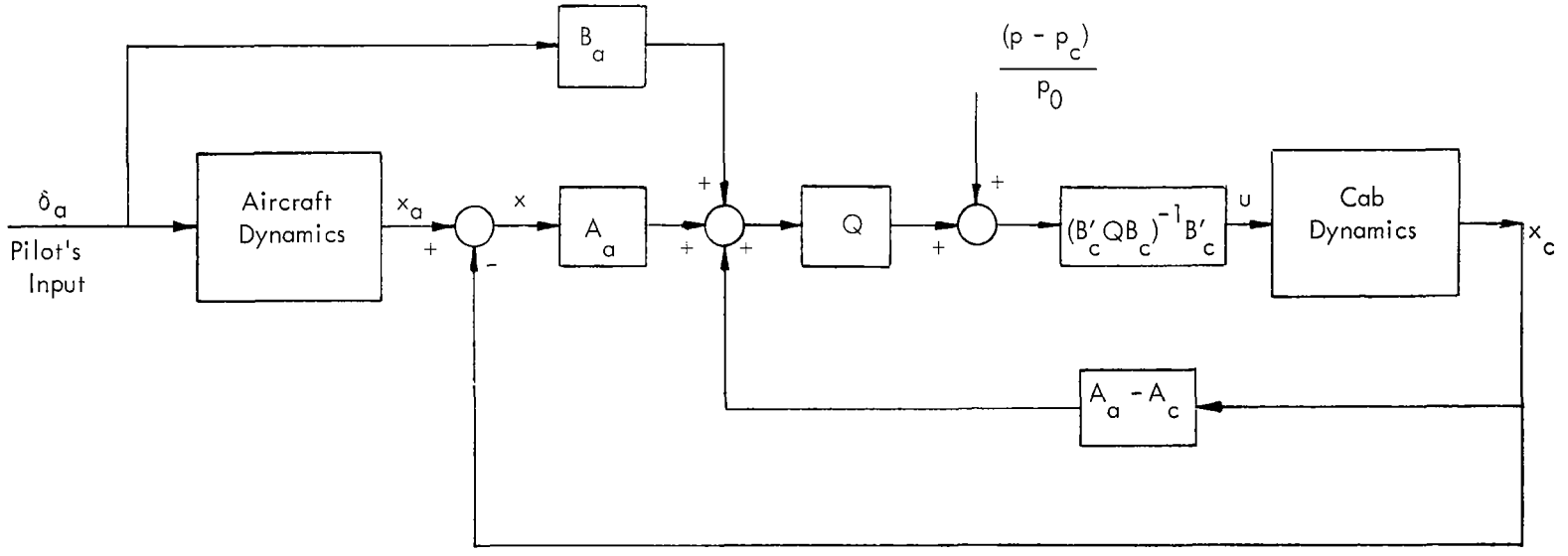

Fig. 3-1

Structure of Optimum Control System

$$\begin{bmatrix} \dot{x}_c \\ \dot{x} \\ \hline \dot{p}_c \\ \dot{p} \end{bmatrix} = \left[\begin{array}{cc:cc} A_{11} & A_{12} & B_{11} & -B_{11} \\ A_{21} & A_{22} & -B_{11} & B_{11} \\ \hdashline C_{11} & C_{12} & -A'_{11} & -A'_{21} \\ C'_{12} & C_{22} & -A'_{12} & -A'_{22} \end{array}\right] \begin{bmatrix} x_c \\ x \\ \hline p_c \\ p \end{bmatrix} + \begin{bmatrix} R_1 \\ R_2 \\ \hline R_3 \\ R_4 \end{bmatrix} B_a \delta_a + \begin{bmatrix} 0 \\ 0 \\ \hline \epsilon \frac{\partial L}{\partial x_c} \\ 0 \end{bmatrix} \tag{3.26}$$

where p_0 has been equated to -1 and

$$A_{11} = (I - B_c B_c^{\#})A_c + B_c B_c^{\#} A_a$$

$$A_{12} = B_c B_c^{\#} A_a$$

$$A_{21} = (I - B_c B_c^{\#})(A_a - A_c)$$

$$A_{22} = (I - B_c B_c^{\#})A_a$$

$$B_{11} = B_c (B_c' Q B_c)^{-1} B_c'$$

$$C_{11} = (A_a - A_c)' Q [I - B_c B_c^{\#}](A_a - A_c)$$

$$C_{12} = (A_a - A_c)' Q [I - B_c B_c^{\#}] A_a$$

$$C_{22} = A_a' Q [I - B_c B_c^{\#}] A_a$$

$$R_1 = B_c B_c^{\#}$$

$$R_2 = I - B_c B_c^{\#}$$

$$R_3 = (A_a - A_c)' Q [I - B_c B_c^{\#}]$$

$$R_4 = A_a' Q [I - B_c B_c^{\#}]$$

and $B_c^{\#}$ is a "pseudo inverse" of B_c with respect to the matrix Q, i.e.

$$B_c^{\#} = (B_c' Q B_c)^{-1} B_c' Q$$

where $B_c^{\#} B_c = I$

Two features of (3.26) are specially noteworthy:

(1) Owing to the presence of the term $\epsilon \partial L/\partial x_c$, the equations are nonlinear. This problem is overcome by use of the quasi-optimum control technique in which $\partial L/\partial x_c$ will be computed for $\epsilon = 0$ and B_c nonsingular.

(2) The pilot's imput δ_a appears as a forcing function. Since the determination of $p(t) - p_c(t)$ at the "present time" t requires solving (3.26) for future times $(t \leq \tau \leq T+t)$ it is clear that a knowledge of $\delta_a(\tau)$ in the future might be necessary. We will return to this problem in the sequel.

3.2 General Solution of the "Simplified Problem"

The "simplified problem" for the application of the quasi-optimum control technique is obtained from (3.26) by setting $\epsilon = 0$. It is readily demonstrated that the solution to (3.26) can be expressed as

$$-\begin{bmatrix} p_c \\ \hline p \end{bmatrix} = M \begin{bmatrix} x_c \\ \hline x \end{bmatrix} + y(\delta_a(\cdot)) \tag{3.27}$$

where M satisfies a matrix Riccati equation and y is a linear functional of $\delta_a(\tau)$ for $t \leq \tau \leq T+t$. The special structure of the matrices in (3.26) permit the use of a special method of solution. For this purpose, it is noted that the contribution from p_c and p to the optimum control law depends only on

$$z = p_c - p \tag{3.28}$$

From (3.27) it follows that

$$-z = N_c x_c + Nx + q \tag{3.29}$$

where N_c and N are submatrices of M and q is a subvector of y. We shall obtain differential equations for N_c, N, and q.

From (3.29) we have

$$-\dot{z} = \dot{N}_c x_c + N_c \dot{x}_c + \dot{N}x + N\dot{x} + \dot{q} \tag{3.30}$$

But, from (3.26)

$$\begin{aligned}\dot{x}_c &= A_{11}x_c + A_{12}x + B_{11}z + R_1 B_a \delta_a \\ &= A_{11}x_c + A_{12}x - B_{11}(N_c x_c + Nx + q) + R_1 B_a \delta_a\end{aligned}$$

and

$$\begin{aligned}\dot{x} &= A_{21}x_c + A_{22}x - B_{11}z + R_2 B_a \delta_a \\ &= A_{21}x_c + A_{22}x + B_{11}(N_c x_c + Nx + q) + R_2 B_a \delta_a\end{aligned}$$

Whence (3.30) becomes

$$\begin{aligned}-\dot{z} = \dot{N}_c x_c &+ N_c[(A_{11} - B_{11}N_c)x_c + (A_{12} - B_{11}N)x - B_{11}q + R_1 B_a \delta_a] \\ &+ \dot{N}x + N[(A_{21} + B_{11}N_c)x_c + (A_{22} + B_{11}N)x + B_{11}q + R_2 B_a \delta_a] + \dot{q}\end{aligned} \tag{3.31}$$

Also from (3.26) with $\epsilon = 0$

$$\dot{p}_c - \dot{p} = \dot{z} = (C_{11} - C'_{12})x_c + (C_{12} - C_{22})x - (A_{11} - A_{12})'p_c$$
$$- (A_{21} - A_{22})'p + (R_3 - R_4)B_a\delta_a \tag{3.32}$$

Now

$$A_{11} - A_{12} = (I - B_c B_c^{\#})A_c = \tilde{A}_c = -(A_{21} - A_{22})$$

Hence (3.32) becomes

$$\dot{z} = (C_{11} - C'_{12})x_c + (C_{12} - C_{22})x - \tilde{A}'_c z + (R_3 - R_4)B_a\delta_a \tag{3.33}$$
$$= (C_{11} - C'_{12})x_c + (C_{12} - C_{22})x + \tilde{A}'_c[N_c x_c + Nx + q] + (R_3 - R_4)B_a\delta_a$$
$$= (C_{11} - C'_{12} + \tilde{A}'_c N_c)x_c + (C_{12} - C_{22} + \tilde{A}'_c N)x + \tilde{A}'_c q + (R_3 - R_4)B_a\delta_a$$

Adding (3.31) and (3.33) results in

$$0 = [\dot{N}_c + N_c(A_{11} - B_{11}N_c) + N(A_{21} + B_{11}N_c) + C_{11} - C'_{12} + \tilde{A}'_c N_c]x_c$$
$$+ [\dot{N} + N_c(A_{12} - B_{11}N) + N(A_{22} + B_{11}N) + C_{12} - C_{22} + \tilde{A}'_c N]x$$
$$+ [(N - N_c)B_{11} + \tilde{A}'_c]q + (N_c R_1 + NR_2 + R_3 - R_4)B_a\delta_a + \dot{q}$$

This must hold for all x and x_c. Hence we must have

$$\dot{N}_c + N_c A_{11} + NA_{21} - N_c B_{11} N_c + NB_{11} N_c + C_{11} - C'_{12} + \tilde{A}'_c N_c = 0 \tag{3.34}$$

$$\dot{N} + N_c A_{12} + NA_{22} - N_c B_{11} N + NB_{11} N + C_{12} - C_{22} + \tilde{A}'_c N = 0 \tag{3.35}$$

$$\dot{q} + [\tilde{A}'_c + (N - N_c)B_{11}]q + (N_c R_1 + NR_2 + R_3 - R_4)B_a\delta_a = 0 \tag{3.36}$$

Subtract (3.35) from (3.34) to obtain

$$\dot{N}_c - \dot{N} + N_c(A_{11} - A_{12}) + N(A_{21} - A_{22}) - (N_c - N)B_{11}(N_c - N)$$

$$+ C_{11} - C'_{12} - C_{12} + C_{22} + \tilde{A}'_c(N_c - N) = 0$$

or, letting $F = N_c - N$

$$\dot{F} + F\tilde{A}_c + \tilde{A}'_c F - FB_{11}F + C_{11} - C'_{12} - C_{12} + C_{22} = 0 \tag{3.37}$$

Now

$$C_{11} - C'_{12} = - A'_c Q[I - B_c B_c^{\#}](A_a - A_c)$$

$$C_{22} - C_{12} = + A'_c Q[I - B_c B_c^{\#}]A_a$$

Hence (3.37) becomes

$$-\dot{F} = F\tilde{A}_c + \tilde{A}'_c F - FB_{11}F + A'_c Q[I - B_c B_c^{\#}]A_c \tag{3.38}$$

which is an nxn Riccati equation. The solution F of this equation can be substituted into (3.34) or (3.35) to obtain linear equations for N or N_c. In particular,

$$-\dot{N} = NA_a + (\tilde{A}'_c - FB_{11})N + C_{12} - C_{22} - FA_{22} \tag{3.39}$$

$$-\dot{N}_c = N_c A_a + (\tilde{A}'_c - FB_{11})N_c + C_{11} - C'_{12} - FA_{21} \tag{3.40}$$

If the terminal state $\{x_c(T + t),\ x(T + t)\}$ is free then $p_c(T + t) = p(T + t) = 0$, $N(T + t) = N_c(T + t) = F(T + t) = 0$ is the terminal condition which should be used for the backward integration of (3.38) and (3.39) or (3.40).

Also, from (3.36)

$$q(t) = \int_{t}^{T+t} \Phi'(s, t)\{FB_c B_c^{\#} + N - A'_c Q[I - B_c B_c^{\#}]\} B_a \delta_a(s)\, ds \qquad (3.41)$$

where $\Phi'(s, t)$ is the state-transition matrix corresponding to $\tilde{A}_c - B_{11} F$.

It is noted that the matrix M and the function y in (3.27), that are characterized by N_c, N and q, respectively, in (3.29), are time varying for any fixed terminal time T as can be seen from the solutions of (3.38) - (3.41). Consequently, the optimum control law for the "simplified" system (will be referred to as "simplified control") is also explicitly time dependent for finite T. As this is somewhat undesirable from a practical point of view, in subsequent applications of the theory developed therein, it will be assumed that $T \to \infty$ so that $\dot{F} = \dot{N} = \dot{N}_c = 0$.

The block diagram for the simplified control system is shown in Fig. 3-2.

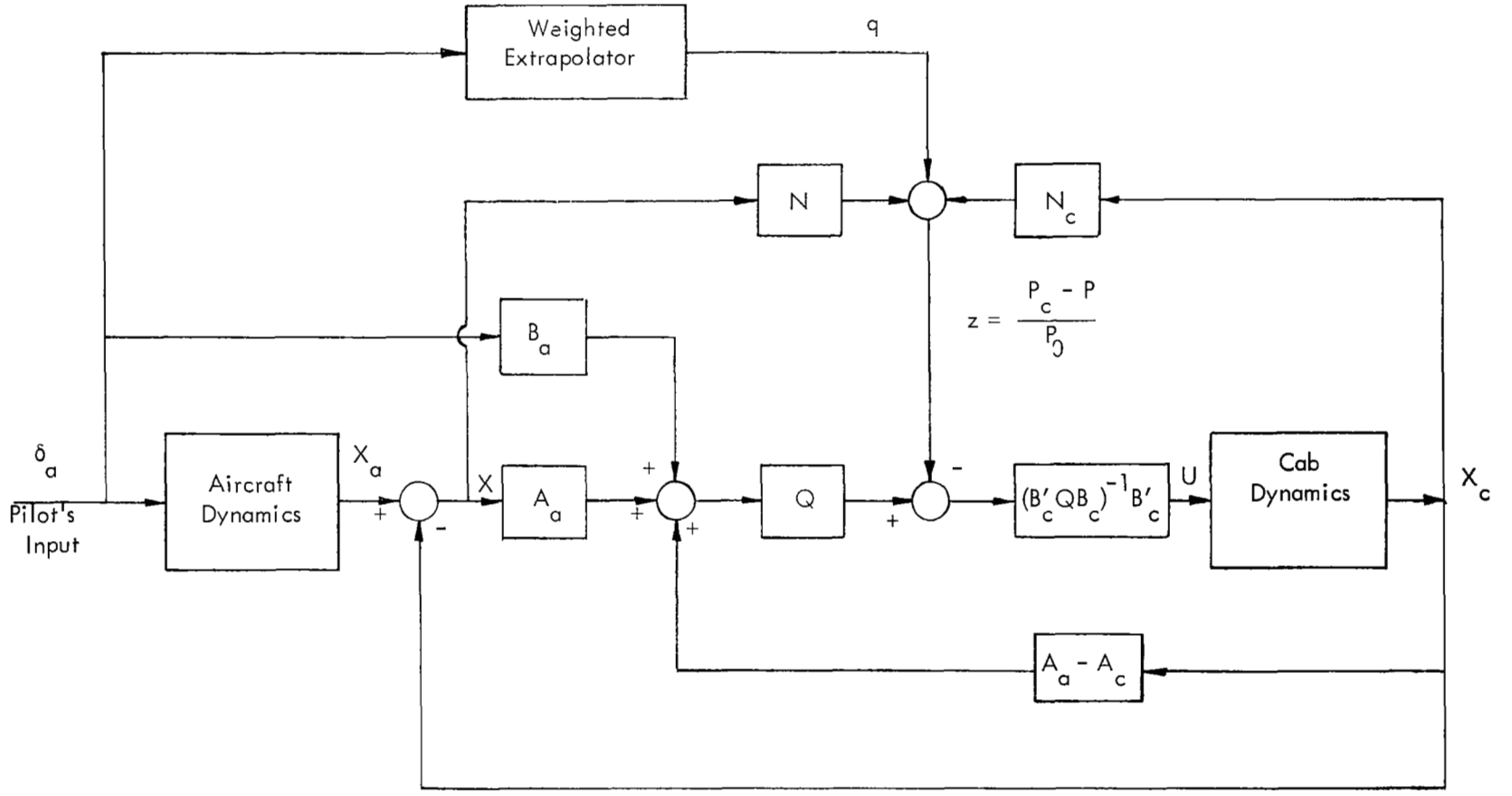

Fig. 3-2

Structure of Simplified Controller

3.3 Quasi-Optimum Control Law Using Hamilton-Jacobi Equation

Substitution of the optimum control law (3 23) into the Hamiltonian (3.12) results in the following expression

$$h = p_0 [\frac{1}{2} (A_{21}x_c + A_{22}x + R_2 B_a \delta_d^\gamma Q(A_{21}x_c + A_{22}x + R_2 B_{aa}\delta) + \epsilon L(x_c)]$$

$$- \frac{1}{2p_0} (p_c - p)' B_{11} (p_c - p) + p_c' (A_{11}x_c + A_{12}x) + p'(A_{21}x_c + A_{22}x) \qquad (3.42)$$

$$+ (p_c' R_1 + p' R_2) B_{aa}\delta + p_\tau$$

Equating the Hamiltonian h to zero and setting $p_0 = -1$ results in the Hamilton-Jacobi equation when the following identification is made:

$$p_c = -\frac{\partial v}{\partial x_c}$$

$$p = -\frac{\partial v}{\partial x}$$

$$p_\tau = -\frac{\partial v}{\partial \tau}$$

where

$$v = v(x_c(\tau), x(\tau), \tau) = \text{optimum value of performance integral} \qquad (3.4)$$

Following the procedure used in NASA CR-1099 ("Additional Studies of Quasi-Optimum Feedback Control Techniques"), Part 1, Section 1.1, v is written as

$$v = V + \epsilon W + O(\epsilon^2) \qquad (3.43)$$

Hence

$$p_c = -\frac{\partial V}{\partial x_c} - \epsilon \frac{\partial W}{\partial x_c} + O(\epsilon^2)$$

$$p = -\frac{\partial V}{\partial x} - \epsilon \frac{\partial W}{\partial x} + O(\epsilon^2) \qquad (3.44)$$

$$p_\tau = -\frac{\partial V}{\partial \tau} - \epsilon \frac{\partial W}{\partial \tau} + O(\epsilon^2)$$

Let

$$P_c = -\frac{\partial V}{\partial x_c}$$

$$P = -\frac{\partial V}{\partial x}$$

$$P_\tau = -\frac{\partial V}{\partial \tau}$$

Then the Hamilton-Jacobi equation becomes:

$$\begin{aligned} 0 = & -\frac{1}{2}(A_{21}x_c + A_{22}x + R_2 B_{a\alpha}\delta)' Q(A_{21}x_c + A_{22}x + R_2 B_{a\alpha}\delta) + \frac{1}{2}(P_c - P)' B_{11}(P_c - P) \\ & + P_c'(A_{11}x_c + A_{12}x) + P'(A_{21}x_c + A_{22}x) + (P_c'R_1 + P'R_2)B_{a\alpha}\delta + P_\tau \\ & + \epsilon \left\{ -L(x_c) - \left(\frac{\partial W}{\partial x_c} - \frac{\partial W}{\partial x}\right)' B_{11}(P_c - P) - \left(\frac{\partial W}{\partial x_c}\right)'(A_{11}x_c + A_{12}x) \right. \\ & \left. - \left(\frac{\partial W}{\partial x}\right)'(A_{21}x_c + A_{22}x) - \left[\left(\frac{\partial W}{\partial x_c}\right)' R_1 + \left(\frac{\partial W}{\partial x}\right)' R_2\right] B_{a\alpha}\delta - \frac{\partial W}{\partial t} \right\} + O(\epsilon^2) \end{aligned} \qquad (3.45)$$

By ignoring the terms of $O(\epsilon^2)$ and equating the coefficients of ϵ^0 and ϵ individually to zero we obtain two separate equations:

$$0 = -\frac{1}{2}(A_{21}x_c + A_{22}x + R_2 B_a \delta_a)'Q(A_{21}x_c + A_{22}x + R_2 B_a \delta_a) + \frac{1}{2}(P_c - P)' B_{11}(P_c - P)$$

$$+ P_c'(A_{11}x_c + A_{12}x) + P'(A_{21}x_c + A_{22}x) + (P_c'R_1 + P'R_2)B_a\delta_a + P_\tau \tag{3.46}$$

and

$$0 = -L(x_c) - \left(\frac{\partial W}{\partial x_c}\right)'[A_{11}x_c + A_{12}x + B_{11}(P_c - P) + R_1 B_a \delta_a]$$

$$- \left(\frac{\partial W}{\partial x}\right)'[A_{21}x_c + A_{22}x - B_{11}(P_c - P) + R_2 B_a \delta_a] - \frac{\partial W}{\partial \tau} = 0 \tag{3.47}$$

Now (3.46) is precisely the Hamilton-Jacobi equation for the simplified problem of the previous section. Hence the solution to (3.46), using (3.29), is

$$P_c - P = -(N_c x_c + Nx + q) \tag{3.48}$$

and (3.47) becomes

$$0 = -L(x_c) - \left(\frac{\partial W}{\partial x_c}\right)'[(A_{11} - B_{11}N_c)x_c + (A_{12} - B_{11}N)x + R_1 B_a \delta_a - B_{11}q]$$

$$- \left(\frac{\partial W}{\partial x}\right)'[(A_{21} + B_{11}N_c)x_c + (A_{22} + B_{11}N)x + R_2 B_a \delta_a + B_{11}q] - \frac{\partial W}{\partial \tau} \tag{3.49}$$

The partial differential equation (3.49) can be solved by characteristics, or, equivalently, (3.49) can be interpreted as the partial differential equation for the evaluation of

$$W = \int_t^{T+t} L(x_c)\,dt \tag{3.50}$$

for the <u>closed-loop</u> simplified process

$$\dot{x}_c = (A_{11} - B_{11}N_c)x_c + (A_{12} - B_{11}N)x + R_1 B_a \delta_a - B_{11}q$$

$$\dot{x} = (A_{21} + B_{11}N_c)x_c + (A_{22} + B_{11}N)x + R_2 B_a \delta_a + B_{11}q \tag{3.51}$$

Letting

$$z_c = -\frac{\partial W}{\partial x_c} \qquad z = -\frac{\partial W}{\partial x}$$

the "adjoint equations" for the new minimization problem (3.50) and (3.51) are:

$$\dot{z}_c = -(A_{11} - B_{11}N_c)'z_c - (A_{21} + B_{11}N_c)'z + \frac{\partial L}{\partial x_c} \tag{3.52}$$

$$\dot{z} = -(A_{12} - B_{11}N)'z_c - (A_{22} + B_{11}N)'z \tag{3.53}$$

The boundary condition is

$$z_c(T + t) = z(T + t) = 0 \tag{3.54}$$

Since the optimum control law depends on

$$p_c - p \cong P_c - P + \epsilon[z_c - z]$$

we need only the differential equation for

$$\rho = z_c - z \tag{3.55}$$

Upon subtraction of (3.52) from (3.53), we obtain

$$\dot{\rho} = -(\tilde{A}_c - B_{11}F)'\rho + \frac{\partial L}{\partial x_c} \tag{3.56}$$

Let $\Psi(T + t, t)$ be the transition matrix corresponding to $-(\tilde{A}_c - B_{11}F)'$. Then the solution to (3.56) can be written

$$\rho(T + t) = \Psi(T + t, t)\rho(t) + \int^{T+t} \Psi(T + t, s) \frac{\partial L}{\partial x_c(s)}\, ds$$

But, by (3.54), $\rho(T + t) = 0$. Hence

$$\rho(t) = -\int_{t}^{T+t} \Psi(t,s) \frac{\partial L}{\partial x_c(s)}\, ds$$
$$= -\int_{t}^{T+t} \Phi'(s,\, t) \frac{\partial L}{\partial x_c(s)}\, ds \qquad (3.57)$$

where Φ is the transition matrix of the adjoint system $\tilde{A}_c - B_{11} F$.

In order to evaluate (3.57) it is necessary first to integrate (3.51) for $x_c(s)$, then compute $\partial L/\partial x_c(s)$, substitute this result into (3.57) and evaluate, the integral which is a nonlinear functional of $x_c(\cdot)$.

With $T \to \infty$, as discussed in preceeding subsection

$$\rho(t) = -\int_{t}^{\infty} \Phi'(s,\, t) \frac{\partial L}{\partial x_c(s)}\, ds$$

In the calculation of $\rho(t)$ discussed subsequently, it will be convenient to retain the more general case of (3.57) with T = const., and, without loss of generality, $t = 0$.

3.4 Extrapolation of Pilot's Input

It was noted at several occasions in the preceding sections the necessity of extrapolating the pilot's input $\delta_a(\cdot)$ into the future. This extrapolation problem is crucial in the entire design approach, because the need for "washout" feedback depends on the future pilot's input. For example, if the motion limit has nearly been approached, and the pilot continues the same command, the limit will be reached; on the other hand, if the pilot reverses the control, the motion limit may not be reached. The pilot's action, of course, depends on the aircraft motion he desires and is taken (in a realistic simulation) independent of the cab motion, which ought to be unknown to the pilot. Various methods of extrapolating the pilot's action are conceivable; the following have been studied.

(a) Taylor's series expansion of $\delta_a(\tau)$ about the present value $\delta_a(t)$

$$\delta_a(t+\tau) = \delta_a(t) + \tau\dot{\delta}_a(t) + \frac{\tau^2}{2}\ddot{\delta}_a(t) + \frac{\tau^3}{6}\dddot{\delta}_a(t) + \cdots \tag{3.58}$$

(b) Exponential approximation by

$$\delta_a(\tau) = \delta_a(t)\, e^{-k(\tau - t)} \tag{3.59}$$

where k is determined empirically.

(c) For each situation to be simulated (training exercise) determine the action which would or ought to be taken by an experienced pilot and program the corresponding $\delta_a(\tau)$, for the purpose of determining the washout feedback only.

(d) Assume a dynamic model for $\delta_a(\tau)$, i.e. that $\delta_a(\tau)$ satisfies a known differential equation with random excitation, and use a Kalman filtering technique to extrapolate $\delta_a(\tau)$ into the future.

A combination of (c) and (d) can also be used by assuming that $\delta_a(\tau) = \delta_{a_o}(\tau) + \delta_{a_e}(\tau)$ where $\delta_{a_o}(\tau)$ is the nominal action and $\delta_{a_e}(\tau)$ is the difference between the pilot's action and the ideal action.

Of these possible candidates for $\delta_a(\cdot)$ extrapolation, the exponential approximation (b) was found to give favorable results and was used extensively in the investigation.

4. PRACTICAL APPLICATION TO A LONGITUDINAL MOTION SIMULATION

As an application of the general design technique developed in the preceding sections, we considered the longitudinal motion of a present-day transport aircraft whose dynamic equations at C.G. were shown in (2.5) and repeated below.

$$\ddot{y}_a = -a_a \dot{y}_a + b_a \theta_a + c_a \delta_a \tag{4.1a}$$

$$\ddot{\theta}_a = d_a \dot{y}_a - e_a \theta_a - f_a \dot{\theta}_a - g_a \delta_a \tag{4.1b}$$

The corresponding cab dynamics and the various forms of the performance index as defined in Section 2 are rewritten as follows,

$$\ddot{y}_c = -2\xi_1 \omega_1 \dot{y}_c - \omega_1^2 y_c + u_1 \tag{4.2a}$$

$$\ddot{\theta}_c = -2\xi_2 \omega_2 \dot{\theta}_c - \omega_2^2 \theta_c + u_2 \tag{4.2b}$$

$$\begin{aligned} V &= \int_t^{T+t} M(\ddot{e}_y, \dddot{e}_y, \dot{e}_\theta, \ddot{e}_\theta)\, d\tau + \epsilon \int_t^{T+t} L(y_c)\, d\tau \\ &= \frac{1}{2} \int_t^{T+t} (\dot{x}' Q \dot{x})\, d\tau + \epsilon \int_t^{T+t} L(x_c)\, d\tau \end{aligned} \tag{4.3}$$

$$M_1 = \frac{1}{2} (q_{\ddot{y}} \ddot{e}_y^2 + q_{\dot{\theta}} \dot{e}_\theta^2 + q_{\ddot{\theta}} \ddot{e}_\theta^2) \tag{4.4}$$

$$M_2 = \frac{1}{2} (q_{\ddot{y}} \ddot{e}_y^2 + q_{\dddot{y}} \dddot{e}_y^2 + q_{\dot{\theta}} \dot{e}_\theta^2 + q_{\ddot{\theta}} \ddot{e}_\theta^2) \tag{4.5}$$

$$L_1 = \begin{cases} 0 & |y_c| < Y_c \\ |y_c - Y_c| & |y_c| \geq Y_c \end{cases} \tag{4.6}$$

$$L_2 = \left(\frac{y_c}{Y_c} \right)^{2\beta} \qquad \beta \geq 1 \tag{4.7}$$

In computer simulations of the control systems designed, the numerical values of the aircraft parameters were assumed to be as follows:

$$a_a = 0.70$$

$$b_a = 160.0$$

$$c_a = 7.0$$

$$d_a = 0.0034$$

$$e_a = 0.786$$

$$f_a = 0.707$$

$$g_a = 0.69$$

in accordance with data received from Ames Research Center.

In line with the general theory of the preceding section, it is noted that different combinations of the cost function M and the penalty function L result in different control laws u. The combinations (M_1, L_1), (M_1, L_2) and (M_2, L_2) were studied in considerable detail while the combination (M_2, L_1) was relatively unexplored up to the time of this report.

The general design procedure followed entails the steps outlined below:

(1) For any assumed cost function M, obtain the "simplified" control law U with $\epsilon = 0$, using the theory of Section 3.2.

(2) Adjust the parameters in M, so that when U is applied to the cab, the cab motion would approximately duplicate the motion of the aircraft.

(3) With assumed form of the "penalty function" L, calculate the "washout" (i.e. the quasi-optimum correction factor) ρ in accordance with the theory of Section 3.3. Then the optimum control u is given by

$$u \simeq U + \epsilon \rho$$

(4) Adjust ϵ and the parameters in ρ, with U fixed, so that excessive motion due to U is washed out.

(5) Adjust ϵ and those parameters in U and ρ to achieve acceptable acceleration and jerk profiles while maintaining the cab excursion within physical boundary.

It should be noted that since it is impossible in practice to achieve a one-to-one simulation of actual aircraft motion, and since there does not exist an objective performance criterion to assess the relative merit and acceptability of a resulting control system, a "good" result is distinguished from a "bad" result only on the basis of the opinion of those familiar with motion simulators. For this reason the results obtained in each case are presented and discussed.

In all the cases studied, the angular motion of the cab is controlled to follow that of the aircraft exactly since no constraint was imposed on the angular motion. This is because (a) the allowable cab angular motion is large enough to accommodate the corresponding aircraft excursions and (b) no attempt is presently being made to enhance motion perception by intentionally altering the cab angular motion from that of the aircraft. Thus, in our subsequent discussion of the results, attention will be focused on the higher derivatives of translational motion, such as acceleration and/or jerk, and, in particular, on such features as magnitude, phase and "onset" relations between the cab and the aircraft acceleration and/or jerk.

4.1 Control System Design Using Cost Function M_1 Without Jerk Weighting and "Hard" Boundary Penalty Function L_1

In accordance with the state variable notations used in Section 2, let

$$x_{a_1} = y_a \qquad x_{c_1} = y_c$$
$$x_{a_2} = \dot{y}_a \qquad x_{c_2} = \dot{y}_c$$
$$x_{a_3} = \theta_a \qquad x_{c_3} = \theta_c$$
$$x_{a_4} = \dot{\theta}_a \qquad x_{c_4} = \dot{\theta}_c$$

then (4.1) and (4.2) are rewritten as

$$\begin{aligned}
\dot{x}_{a_1} &= x_{a_2} \\
\dot{x}_{a_2} &= -a_a x_{a_2} + b_a x_{a_3} + c_a \delta_a \\
\dot{x}_{a_3} &= x_{a_4} \\
\dot{x}_{a_4} &= d_a x_{a_2} - e_a x_{a_3} - f_a x_{a_4} - g_a \delta_a
\end{aligned} \tag{4.8}$$

and

$$\begin{aligned}
\dot{x}_{c_1} &= x_{c_2} \\
\dot{x}_{c_2} &= -\omega_1^2 x_{c_1} - 2\xi_1 \omega_1 x_{c_2} + u_1 \\
\dot{x}_{c_3} &= x_{c_4} \\
\dot{x}_{c_4} &= -\omega_2^2 x_{c_3} - 2\xi_2 \omega_2 x_{c_4} + u_2
\end{aligned} \tag{4.9}$$

Defining the "error state" x as $x = x_a - x_c$, then the "error dynamics" are obtained from (4.8) and (4.9)

$$\begin{aligned}
\dot{x}_1 &= x_2 \\
\dot{x}_2 &= -a_a x_2 + b_a x_3 + \omega_1^2 x_{c_1} + (2\xi_1\omega_1 - a_a) x_{c_2} + b_a x_{c_3} + c_a \delta_a - u_1 \\
\dot{x}_3 &= x_4 \\
\dot{x}_4 &= d_a x_2 - e_a x_3 - f_a x_4 + d_a x_{c_2} + (\omega_2^2 - e_a) x_{c_3} + (2\xi_2\omega_2 - f_a) x_{c_4} \\
&\quad - g_a \delta_a - u_2
\end{aligned} \tag{4.10}$$

and with the cost function M_1 (4.4), the constant weighting matrix Q for the performance index takes the form

$$Q = \begin{bmatrix} 0 & 0 & 0 & 0 \\ 0 & q_{\dot{y}} & 0 & 0 \\ 0 & 0 & q_{\dot{\theta}} & 0 \\ 0 & 0 & 0 & q_{\ddot{\theta}} \end{bmatrix} \tag{4.11}$$

Thus, the optimal control law (3.23) becomes

$$\begin{aligned}
u_1 &= -a_a x_2 + b_a x_3 + \omega_1^2 x_{c_1} + (2\xi_1\omega_1 - a_a) x_{c_2} + b_a x_{c_3} + c_a \delta_a + \frac{1}{q_{\dot{y}}} (p_{c_2} - p_2) \\
u_2 &= d_a x_2 - e_a x_3 - f_a x_4 + d_a x_{c_2} + (\omega_2^2 - e_a) x_{c_3} + (2\xi_2\omega_2 - f_a) x_{c_4} - g_a \delta_a + \frac{1}{q_{\ddot{\theta}}} (p_{c_4} - p_4)
\end{aligned} \tag{4.12}$$

where p, p_c are the corresponding adjoint variables as defined in Section 3. It was shown that an exact solution of p and p_c from the canonical equations (3.26) is in general very complicated due to the presence of nonlinear "penalty" function term $\epsilon \frac{\partial L(x_c)}{\partial x_c}$. An approximate solution of p and p_c by quasi-optimum technique yields

$$p_c - p = P_c - P + \epsilon \rho \tag{4.13}$$

where P_c, P are the corresponding adjoint variables of the "simplified" system and ρ is the quasi-optimum correction factor. In the following, we shall determine P_c, P and ρ and discuss the approximation techniques employed.

It was shown in Section 3.2 that a solution of the adjoint variables P, P_c for the simplified system with $\epsilon = 0$ is given by

$$-(P_c - P) = N_c X_c + NX + q(t) \tag{4.14}$$

where the matrices N_c and N are obtained by asymptotic solutions of (3.38) and (3.39), where $\dot{F}$ and $\dot{N}$ are set to zero by letting $T \to \infty$,

$$N = \begin{bmatrix} 0 & 0 & 0 & 0 \\ 0 & 0 & 0 & 0 \\ 0 & 0 & 0 & 0 \\ 0 & N_{42} & N_{43} & N_{44} \end{bmatrix} \tag{4.15}$$

$$N_c = \begin{bmatrix} 0 & 0 & 0 & 0 \\ 0 & 0 & 0 & 0 \\ 0 & 0 & 0 & 0 \\ 0 & N_{42} & N_{43} & (\sqrt{q_{\dot{\theta}}\, q_{\ddot{\theta}}} + N_{44}) \end{bmatrix}$$

with

$$N_{44} = \frac{q_{\dot\theta}\sqrt{q_{\dot\theta}/q_{\ddot\theta}}}{\dfrac{d_a b_a}{(a_a + \sqrt{q_{\dot\theta}/q_{\ddot\theta}})} - \sqrt{q_{\dot\theta}/q_{\ddot\theta}}\ (f_a + \sqrt{q_{\dot\theta}/q_{\ddot\theta}}) - e_a}$$

$$N_{43} = (f_a + \sqrt{q_{\dot\theta}/q_{\ddot\theta}})\, N_{44} + q_{\dot\theta} \tag{4.16}$$

$$N_{42} = \frac{d_a}{(a_a + \sqrt{q_{\dot\theta}/q_{\ddot\theta}})}\, N_{44}$$

and the time-dependent $q(t)$ is obtained from (3.41) by integrating backward time

$$q(t) = \begin{bmatrix} 0 \\ 0 \\ 0 \\ q_4(t) \end{bmatrix} \tag{4.17}$$

$$q_4(t) = [c_a N_{42} - g_a(\sqrt{q_{\dot\theta}\, q_{\ddot\theta}} + N_{44})] \int_t^{T+t\sqrt{q_{\dot\theta}/q_{\ddot\theta}}} e^{(t-s)}\, \delta_a(s)\, ds \tag{4.18}$$

It is seen from (4.18) that the determination of $q_4(t)$ at the "present time" t requires the knowledge of $\delta_a(\cdot)$ over the "future time" τ $(t \le \tau \le T)$. Thus, in order to obtain a physically realizable controller, it is necessary to devise some extrapolation scheme to predict $\delta_a(\cdot)$ in the future. A prerequisite in the choice of a prediction technique is that of simplicity, since a closed-form solution is desired for purposes of implementation. Among the possible candidates mentioned in Section 3, the one that appeared most attractive from the viewpoint of simplicity is the exponential form

$$\delta_a(\tau) = \delta_a(t)\, e^{-k(\tau - t)} \tag{4.19}$$

where k is an empirically-determined constant. It will be seen in the sequel that the approximation (4.19) actually provides satisfactory performance and enables the feedback control law to be mission-independent.

Substitution of (4.19) into (4.18) and complete the integration yields

$$q_4(t) = \frac{-c_a N_{42} + g_a(\sqrt{q_{\dot\theta} q_{\ddot\theta}} + N_{44})}{k + \sqrt{q_{\dot\theta}/q_{\ddot\theta}}} \left[e^{-(\sqrt{q_{\dot\theta}/q_{\ddot\theta}} + k)T} - 1 \right] \delta_a(t)$$

and with $T \to \infty$, we have

$$q_4(t) = \frac{-c_a N_{42} + g_a(\sqrt{q_{\dot\theta} q_{\ddot\theta}} + N_{44})}{k + \sqrt{q_{\dot\theta}/q_{\ddot\theta}}} \delta_a(t) \tag{4.20}$$

It is noted in Section 3.3 that a complete solution of the simplified system is necessary in order to evaluate the quasi-optimum correction factor ρ. The "simplified" control is obtained by substituting (4.14) - (4.20) into (4.12):

$$U_1 = -a_a X_2 + b_a X_3 + \omega_1^2 X_{c_1} + (2\xi_1\omega_1 - a_a) X_{c_2} + b_a X_{c_3} + c_a \delta_a$$

$$U_2 = (d_a - \frac{N_{42}}{q_{\ddot\theta}}) X_2 - (e_a + \frac{N_{43}}{q_{\ddot\theta}}) X_3 - (f_a + \frac{N_{44}}{q_{\ddot\theta}}) X_4 + (d_a - \frac{N_{42}}{q_{\ddot\theta}}) X_{c_2} \tag{4.21}$$

$$+ (\omega_2^2 - e_a - \frac{N_{43}}{q_{\ddot\theta}}) X_{c_3} + (2\xi_2\omega_2 - f_a - \frac{N_{44} + \sqrt{q_{\dot\theta} q_{\ddot\theta}}}{q_{\ddot\theta}}) X_{c_4} - g_a \delta_a - \frac{q_4}{q_{\ddot\theta}}$$

Substituting (4 21) into (4.9), and using the relation $X = x_a - X_c$ to eliminate the error state X, we obtain the closed-loop "simplified" system equations for the cab.

$$
\begin{aligned}
\dot{X}_{c_1} &= X_{c_2} \\
\dot{X}_{c_2} &= -a_a x_{a_2} + b_a x_{a_3} + c_a \delta_a \\
\dot{X}_{c_3} &= X_{c_4} \\
\dot{X}_{c_4} &= -\sqrt{q_{\dot\theta}/q_{\ddot\theta}}\; X_{c_4} + (d_a - \frac{N_{42}}{q_{\ddot\theta}}) x_{a_2} - (e_a + \frac{N_{43}}{q_{\ddot\theta}}) x_{a_3} \\
&\quad - (f_a + \frac{N_{44}}{q_{\ddot\theta}}) x_{a_4} - g_a \delta_a - \frac{q_4}{q_{\ddot\theta}}
\end{aligned}
\tag{4.22}
$$

Or, in view of the aircraft dynamics (4.8), (4.22) can be rewritten as

$$
\begin{aligned}
\dot{X}_{c_1} &= X_{c_2} \\
\dot{X}_{c_2} &= \dot{x}_{a_2} \\
\dot{X}_{c_3} &= X_{c_4} \\
\dot{X}_{c_4} &= \dot{x}_{a_4} - \sqrt{q_{\dot\theta}/q_{\ddot\theta}}\; X_{c_4} - \frac{N_{42}}{q_{\ddot\theta}} x_{a_2} - \frac{N_{43}}{q_{\ddot\theta}} x_{a_3} \\
&\quad - \frac{N_{44}}{q_{\ddot\theta}} x_{a_4} - \frac{q_4}{q_{\ddot\theta}}
\end{aligned}
\tag{4.23}
$$

It is seen from (4.23) that the simplified control results in a complete "cancellation" of cab dynamics and, for the translational motion (X_{c_1} , X_{c_2}) in particular, substitutes the aircraft dynamics in its place. It can be seen from (4.16) and (4.18) that the weighting coefficients $q_{\dot\theta}$ and $q_{\ddot\theta}$ appear in the expressions for the terms $N_{42}/q_{\ddot\theta}$, $N_{43}/q_{\ddot\theta}$, $N_{44}/q_{\ddot\theta}$, $q_4/q_{\ddot\theta}$ in terms of their ratio $q_{\dot\theta}/q_{\ddot\theta}$ and that all these terms may vanish as $q_{\dot\theta}/q_{\ddot\theta} \to 0$. Thus, it would appear that, since there is no limitation to the angular motion, the ratio $q_{\dot\theta}/q_{\ddot\theta}$ can be set to 0 to allow a perfect angular motion (X_{c_3} , X_{c_4}) simulation. In other words, the simplified control law forces the cab to "duplicate" the motion of the aircraft, disregarding the

physical boundaries. It will be shown in the following that the "excessive" cab motion is to be "washed out" by the correction factor ρ derived in accordance with the framework of the quasi-optimum control technique.

In Section 3.3 it was found that the correction factor ρ, which accounts for the difference between the adjoint variables $(p_c - p)$ and $(P_c - P)$ of the exact and simplified systems respectively, can be obtained by solving (3.56), which, for the present example, is

$$\begin{aligned}
\dot{\rho}_1 &= \frac{\partial L(X_c)}{\partial X_{c_1}} \\
\dot{\rho}_2 &= -\rho_1 \\
\dot{\rho}_3 &= 0 \\
\dot{\rho}_4 &= -\rho_3 - \sqrt{q_{\dot{\theta}}/q_{\ddot{\theta}}}\ \rho_4
\end{aligned} \tag{4.24}$$

with $\rho(T) = 0$. Thus solutions of (4.24) requires an appropriate choice of the "penalty" function $L(X_c)$ and an explicit time solution of X_c from (4.22) and (4.8).

It is immediately clear from (4.24) and the boundary conditions $\rho(T) = 0$ that,

$$\rho_3(t) = \rho_4(t) \equiv 0 \tag{4.25}$$

which is intuitively obvious, since, as noted in the beginning of Section 4, no limitation was imposed on, and, therefore, no washout is necessary for angular motion, hence

$$\rho(t) = \begin{bmatrix} \rho_1(t) \\ \rho_2(t) \\ 0 \\ 0 \end{bmatrix} \tag{4.26}$$

Thus, substitution of (4.26) and (4.14) into (4.13) and subsequently into (4.12) yields the quasi-optimum control law.

$$u_1 \simeq -a_a x_2 + b_a x_3 + \omega_1^2 x_{c_1} + (2\xi_1\omega_1 - a_a)\, x_{c_2} + b_a x_{c_3} + c_a \delta_a + \frac{\epsilon}{q_{\ddot{y}}}\, \rho_2$$

$$u_2 \simeq (d_a - \frac{N_{42}}{q_{\ddot{\theta}}})\, x_2 - (e_a + \frac{N_{43}}{q_{\ddot{\theta}}})\, x_3 - (f_a + \frac{N_{44}}{q_{\ddot{\theta}}})\, x_4 + (d_a - \frac{N_{42}}{q_{\ddot{\theta}}})\, x_{c_2} \qquad (4.27)$$

$$+ (\omega_2^2 - e_a - \frac{N_{43}}{q_{\ddot{\theta}}})\, x_{c_3} + (2\xi_2\omega_2 - f_a - \frac{N_{44} + \sqrt{q_{\dot{\theta}}\, q_{\ddot{\theta}}}}{q_{\ddot{\theta}}})\, x_{c_4} - g_a \delta_a - \frac{q_4}{q_{\ddot{\theta}}}$$

Or, using $x + x_c = x_a$, (4.27) is rewritten as

$$u_1 \simeq \omega_1^2 x_{c_1} + 2\xi_1\omega_1 x_{c_2} - a_a x_{a_2} + b_a x_{a_3} + c_a \delta_a + \frac{\epsilon}{q_{\ddot{y}}}\, \rho_2$$

$$u_2 \simeq \omega_2^2 x_{c_3} + (2\xi_2\omega_2 - \sqrt{q_{\dot{\theta}}/q_{\ddot{\theta}}})\, x_{c_4} + (d_a - \frac{N_{42}}{q_{\ddot{\theta}}})\, x_{a_2} \qquad (4.28)$$

$$-(e_a + \frac{N_{43}}{q_{\ddot{\theta}}})\, x_{a_3} - (f_a + \frac{N_{44}}{q_{\ddot{\theta}}})\, x_{a_4} - g_a \delta_a - \frac{q_4}{q_{\ddot{\theta}}}$$

Substitution of the quasi-optimum control law (4.28) into the cab dynamics (4.9) results in closed-loop quasi-optimum cab system equations.

$$\begin{aligned}
\dot{x}_{c_1} &= x_{c_2} \\
\dot{x}_{c_2} &= \dot{x}_{a_2} + \frac{\epsilon}{q_{\ddot{y}}}\, \rho_2 \\
\dot{x}_{c_3} &= x_{c_4} \\
\dot{x}_{c_4} &= \dot{x}_{a_4} - \sqrt{q_{\dot{\theta}}/q_{\ddot{\theta}}}\; x_{c_4} - \frac{N_{42}}{q_{\ddot{\theta}}}\, x_{a_2} - \frac{N_{43}}{q_{\ddot{\theta}}}\, x_{a_3} - \frac{N_{44}}{q_{\ddot{\theta}}}\, x_{a_4} - \frac{q_4(t)}{q_{\ddot{\theta}}}
\end{aligned} \qquad (4.29)$$

The system equation (4.29), together with the aircraft dynamics (4.8), will be used extensively in the subsequent computer simulation study of assessing the effect of the quasi-optimum wash-out ρ_2.

In the following we shall focus our attention to the calculation of the washout ρ_2.

Calculation of ρ_2 - For $L_1(X_c)$ of (4.6),

$$L_1(X_c) = \begin{cases} 0 & |X_{c_1}| < Y_c \\ |X_{c_1} - Y_c| & |X_{c_1}| \geq Y_c \end{cases}$$

we have

$$\frac{\partial L}{\partial X_{c_1}} = \begin{cases} 0 \quad , & |X_{c_1}| < Y_c \\ \text{sgn}\,(X_{c_1}) \quad , & |X_{c_1}| \geq Y_c \end{cases} \tag{4.30}$$

In order to accommodate the integration of (4.24) with the highly nonlinear term (4.30), we define a "cross-over" time T_c, $t \leq T_c + t \leq T + t$, to denote the time at which the cab position X_{c_1} reaches the physical boundary $\pm Y_c$ and let T_c^+ denote the cross-over time when $X_{c_1} = +Y_c$, and, T_c^- when $X_{c_1} = -Y_c$. The equations of (4.24) are then integrated from t to $T_c + t$ and from $T_c + t$ to $T + t$, to yield

$$\rho_2(t) = \begin{cases} -\frac{1}{2}(T^2 - T_c^{+2}) \\ \frac{1}{2}(T^2 - T_c^{-2}) \end{cases} \tag{4.31}$$

In order to apply the feedback washout, (4.31), to the control (4.28), it is necessary to evaluate T_c analytically. T_c can be obtained by first solving (4.8) and (4.23) for $X_{c_1}(\tau)$ and then let $X_{c_1}(T_c^{\pm}) = \pm Y_c$ to solve for T_c^+ and T_c^-, however, this is rather complicated, and two expedients were employed to evaluate T_c:

(1) The differential equations (4.8) and (4.23) for the vertical displacement was integrated numerically until the displacement exceeded the boundary.

(2) A polynomial approximation

$$X_{c_1}(T_c) = \gamma \dddot{X}_{c_1} T_c^2 + X_{c_1} T_c + X_{c_1} \tag{4.32}$$

was employed, where γ is an adjustable parameter. In other words T_c was found by solving the quadratic equation (4.32) with $X_{c_1}(T_c) = \pm Y_c$ and the least positive root using both $+Y_c$ or $-Y_c$ was taken as the cross-over time.

The resulting trajectories for which the cross-over time T_c was obtained from on-line computer solution of (4.8) and (4.23) are shown in Fig. 4-1, with square pulse input. Fig. 4-2 and 4-3 show some of the resulting trajectories for which the cross-over time T_c was obtained from solving the approximate model (4.32) for various values of γ with the same square pulse input. Various values of the constant parameters $q_{\dddot{y}}$, $q_{\dot{\theta}}$, $q_{\ddot{\theta}}$, ϵ, k, γ, T, Y_c used in the simulation are listed in Table 4-1.

In these figures, the trajectories labeled (a) differ from those of (b) in that heavier washout was applied in (a) by adjusting the constant weighting parameter ϵ so that the cab position can be confined to within ± 10 ft at all times. The cab motions are plotted in solid line, while the corresponding aircraft motions are represented by dashed line.

The error in angular motion (e.g. pitch, pitch rate) is zero in all of those cases. As for the translational motion, it is pointed out by experienced personnel in Ames that the major drawbacks that are common to those trajectories are the presence of jump phenomenon and the inadequate phase relationship in the acceleration profiles. Although no further investigation of this washout technique was pursued, it is believed that use of different cost functions M in conjunction with this penalty function may give better results and worth further investigation.

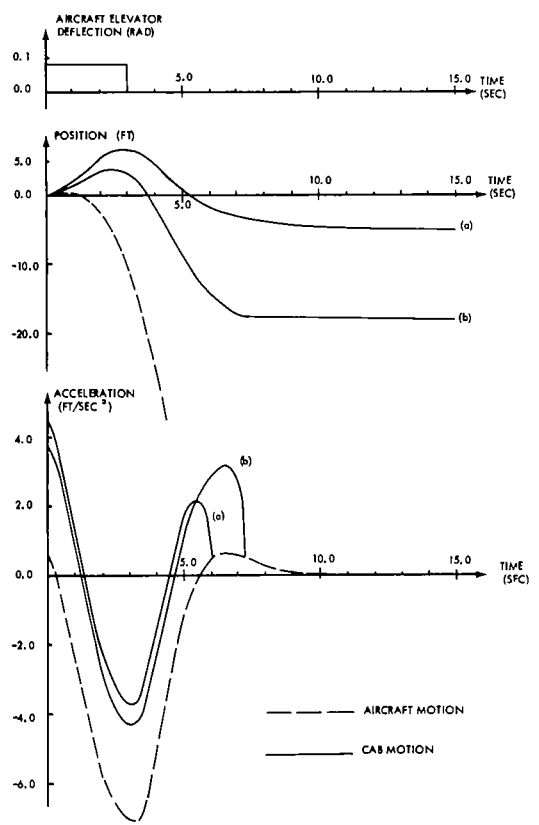

FIGURE 4-1

TRANSIENT RESPONSES FOR CONTROL SYSTEM USING ACCELERATION WEIGHTED COST FUNCTION M_1 AND HARD PENALTY FUNCTION L_1: WITH EXACT ESTIMATION OF CROSS-OVER TIME

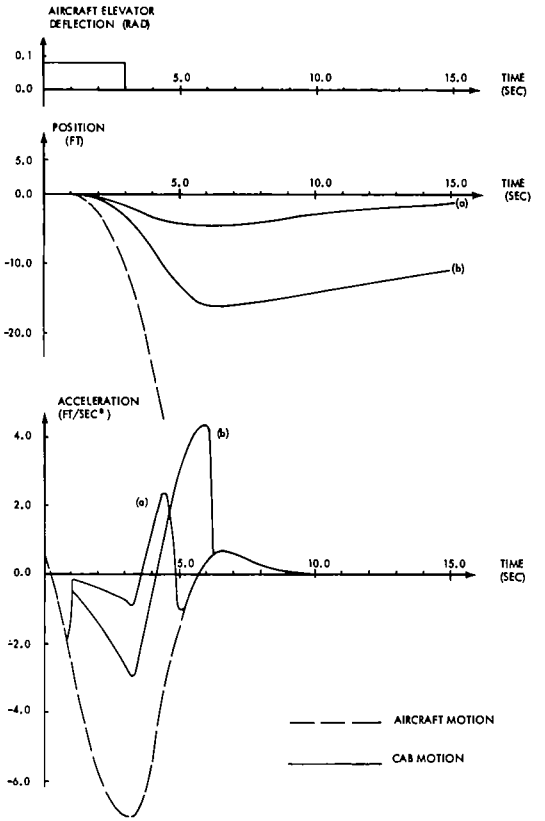

FIGURE 4-2

TRANSIENT RESPONSES FOR CONTROL SYSTEM USING ACCELERATION WEIGHTED COST FUNCTION M_1 AND HARD PENALTY FUNCTION L_1: WITH APPROXIMATE ESTIMATION OF CROSS-OVER TIME (γ=0)

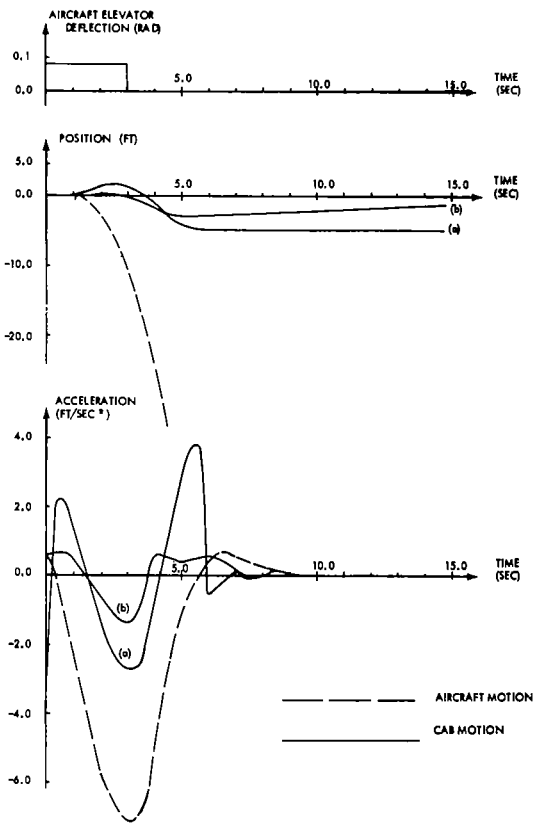

FIGURE 4-3

TRANSIENT RESPONSES FOR CONTROL SYSTEM USING ACCELERATION WEIGHTED COST FUNCTION M_1 AND HARD PENALTY FUNCTION L_1: WITH APPROXIMATE ESTIMATION OF CROSS-OVER TIME ($\gamma \neq 0$)

Table 4-1

Parameters Used in Computer Simulation of Control Scheme (M_1, L_1)

Parameters	Values Used in Figures					
	Figure 4-1		Figure 4-2		Figure 4-3	
	(a)	(b)	(a)	(b)	(a)	(b)
$q_{\ddot{y}}$	10	10	10	10	10	10
$q_{\dot{\theta}}$	0	0	0	0	0	0
$q_{\ddot{\theta}}$	-	-	-	-	-	-
ϵ	0.05	0.025	0.06	0.04	0.04	0.052
k	-	-	-	-	-	-
γ	-	-	0.0	0.0	0.05	0.01
T	40	50	50	50	50	50
Y_c	20	20	20	20	10	10

4.2 Control System Design Using Cost Function M_1 Without Jerk Weighting and "Soft" Boundary Penalty Function L_2

The quasi-optimum control law (4.28) derived in the preceding section also applies in this case because the simplified problems for these two cases are identical. Here we need only calculate the correction factor ρ_2 based on the penalty function L_2.

Calculations of ρ_2:

For $L_2(X_c)$ of (4.7)

$$L_2(X_c) = \left(\frac{X_{c_1}}{Y_c} \right)^{2\beta} \qquad \beta \geq 1$$

we have

$$\frac{\partial L_2}{\partial X_{c_1}} = \frac{2\beta}{Y_c^{2\beta}} X_{c_1}^{(2\beta-1)} \tag{4.33}$$

In order to solve ρ_2 from (4.24) with $\partial L/\partial X_{c_1}$ given by (4.33) it is necessary first to obtain the time solution of X_{c_1} from the closed-loop simplified system (4.23). To simplify the calculation, it is assumed that X_{c_1} is governed by the following second order system

$$\ddot{X}_{c_1} + k_1 \dot{X}_{c_1} = -k_2 \delta_a e^{-k_3(\tau - t)} \tag{4.34}$$

$$k_1 \leq 0, \quad k_2, k_3 \geq 0$$

where k_1, k_2, k_3 are arbitrary constants, and $t \leq \tau \leq T + t$.

Assuming that the present time $t = 0$, the solution of (4.34) yields

$$\begin{aligned} X_{c_1}(\tau) &= \left[X_{c_1} + \frac{1}{k_1} X_{c_2} - \frac{k_2}{k_1 k_3} \delta_a \right] - \left[\frac{1}{k_1} X_{c_2} - \frac{k_2}{k_1(k_3 - k_1)} \delta_a \right] e^{-k_1 \tau} \\ &\quad + \left[\frac{-k_2}{k_3(k_3 - k_1)} \delta_a \right] e^{-k_3 \tau} \\ &= C_1 - C_2 e^{-k_1 \tau} + C_3 e^{-k_3 \tau} \end{aligned} \tag{4.35}$$

where

$$C_1 = X_{c_1} + \frac{1}{k_1} X_{c_2} - \frac{k_2}{k_1 k_3} \delta_a$$

$$C_2 = \frac{1}{k_1} X_{c_2} - \frac{k_2}{k_1(k_3 - k_1)} \delta_a \qquad (4\ 36)$$

$$C_3 = - \frac{k_2}{k_3(k_3 - k_1)} \delta_a$$

Thus substitution of (4.35) into (4.33) and subsequently into (4.24) and carrying out the integration yields:

For $\beta = 1$,

$$\rho_2 = \frac{2}{Y_c^2} \left\{ - \frac{C_1}{2} T^2 - \frac{C_2}{k_1} \left[\left(T + \frac{1}{k_1} \right) e^{-k_1 T} - \frac{1}{k_1} \right] + \frac{C_3}{k_3} \left[\left(T + \frac{1}{k_3} \right) e^{-k_3 T} - \frac{1}{k_3} \right] \right\} \qquad (4.37)$$

Note that since C_i are linear in the state and the control variables, the washout ρ_2 is also linear for fixed T as can be expected for a quadratic performance index V.

For $\beta = 2$,

$$\begin{aligned}
\rho_2 = - \frac{4}{Y_c^4} \Bigg\{ & \frac{C_1^3}{2} T^2 + \frac{C_2^3}{3k_1} \left| \left(T + \frac{1}{3k_1} \right) e^{-3k_1 T} - \frac{1}{3k_1} \right| - \frac{C_3^3}{3k_3} \left| \left(T + \frac{1}{3k_3} \right) e^{-3k_3 T} - \frac{1}{3k_3} \right| \\
& - \frac{3C_1 C_2^2}{2k_1} \left| \left(T + \frac{1}{2k_1} \right) e^{-2k_1 T} - \frac{1}{2k_1} \right| - \frac{3C_1 C_3^2}{2k_3} \left| \left(T + \frac{1}{2k_3} \right) e^{-2k_3 T} - \frac{1}{2k_3} \right| \\
& + \frac{3C_1^2 C_2}{k_1} \left| \left(T + \frac{1}{k_1} \right) e^{-k_1 T} - \frac{1}{k_1} \right| - \frac{3C_1^2 C_3}{k_3} \left| \left(T + \frac{1}{k_3} \right) e^{-k_3 T} - \frac{1}{k_3} \right| \\
& + \frac{3C_2 C_3^2}{k_1 + 2k_3} \left| \left(T + \frac{1}{k_1 + 2k_3} \right) e^{-(k_1 + 2k_3) T} - \frac{1}{k_1 + 2k_3} \right| \qquad (4.38) \\
& - \frac{3C_2^2 C_3}{2k_1 + k_3} \left| \left(T + \frac{1}{2k_1 + k_3} \right) e^{-(2k_1 + k_3) T} - \frac{1}{2k_1 + k_3} \right| \\
& + \frac{6C_1 C_2 C_3}{k_1 + k_3} \left| \left(T + \frac{1}{k_1 + k_3} \right) e^{-(k_1 + k_3) T} - \frac{1}{k_1 + k_3} \right| \Bigg\}
\end{aligned}$$

Here, the washout ρ_2 takes a nonlinear state feedback form as it should be. Typical trajectories generated by the resulting control laws for $\beta = 1$ and $\beta = 2$ are shown in Figures 4-4, 4-5, 4-6 and Figures 4-7, 4-8, 4-9, respectively, for various pilot inputs and for values listed in Table 4-2 of the parameters ϵ, $q_{\dddot{y}}$, $q_{\dot{\theta}}$, $q_{\ddot{\theta}}$, k k_1, k_2, k_3, T, Y_c. In these figures, the cab motions are drawn in solid lines, while the corresponding aircraft motions are represented by dashed lines. Note that the weighting coefficient $q_{\dot{\theta}}$ has been set to 0 so that the angular motion of the cab becomes identical to that of the aircraft's. (Refer to the comment following equation (4.23)). Therefore, only the aircraft's angular motion (pitch and pitch rate) is shown in the figures.

It is seen from these figures that the linear washout ($\beta = 1$) provides a smoother trajectory while the nonlinear washout ($\beta = 2$) provides higher fidelity of the onset of acceleration. In both cases, there is a significant phase error in the sense that the cab acceleration crosses zero at an earlier time than the actual aircraft acceleration.

Because of the fact that the washout component of $\rho_4 = 0$ (4.25), and that q_4, N_{42}, N_{43}, N_{44} depend only on the parameters k, $q_{\dot{\theta}}/q_{\ddot{\theta}}$, it is seen from (4.28) that the quasi-optimum pitch control u_2 is dependent only on k, $q_{\dot{\theta}}/q_{\ddot{\theta}}$. On the other hand, because of the assumption (4.34), the quasi-optimum translational control u_1 (4.27) is seen to be dependent only on the parameters ϵ, $q_{\dddot{y}}$, k_1, k_2, and k_3. Thus, we conclude from the dynamic equations of the cab (4.9) that the translational (x_{c_1}, x_{c_2}) and the angular (x_{c_3}, x_{c_4}) motions of the cab can be controlled "separately" by proper choices of the two sets of parameters: (ϵ, $q_{\dddot{y}}$, k_1, k_2, k_3) and ($k, q_{\dot{\theta}}/q_{\ddot{\theta}}$). One convenient procedure which was followed in this study is: pick a proper set of values of ($k, q_{\dot{\theta}}/q_{\ddot{\theta}}$) so that the angular cab motion follows that of aircraft closely; fix these values and then adjust the set (ϵ, $q_{\dddot{y}}$, k_1, k_2, k_3) till the translational motion is acceptable.

A complete block diagram of the implementation of the control law by means of an analog computer is shown in Fig. 4-10. For preliminary studies, instrumentation of the cab state variables may not be feasible. In this case an "open-loop" implementation can be achieved (at the expense of the benefits of feedback) by realizing a "model" of the cab in the analog computer, and using the state of the model in place of the state of the cab. The implementation is shown in Fig. 4-11.

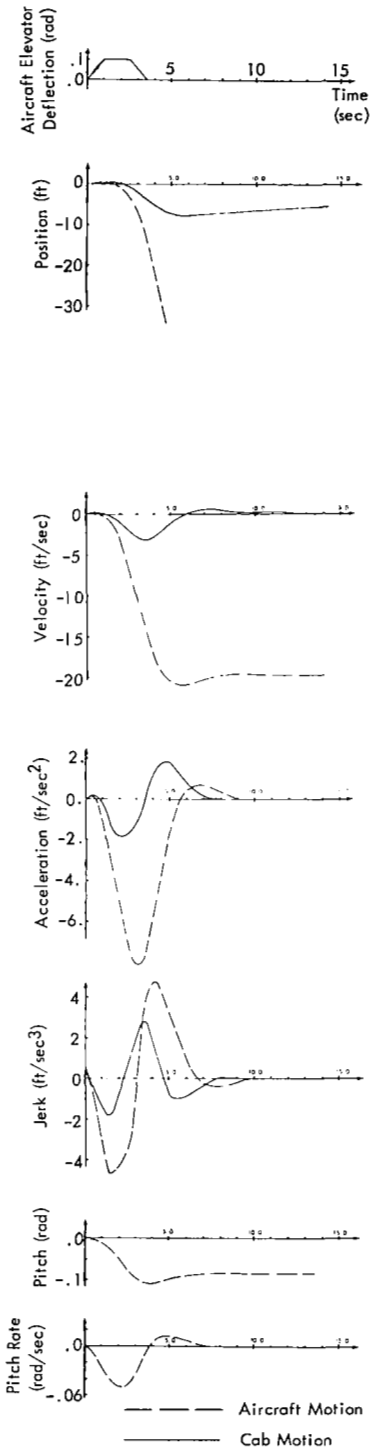

Figure 4-4
Transient Responses for Control System Using Acceleration Weighted Cost Function M_1 and Quadratic Penalty Function $L_2(\beta=1\ 0)$: with Single Trapezoidal Pulse Input

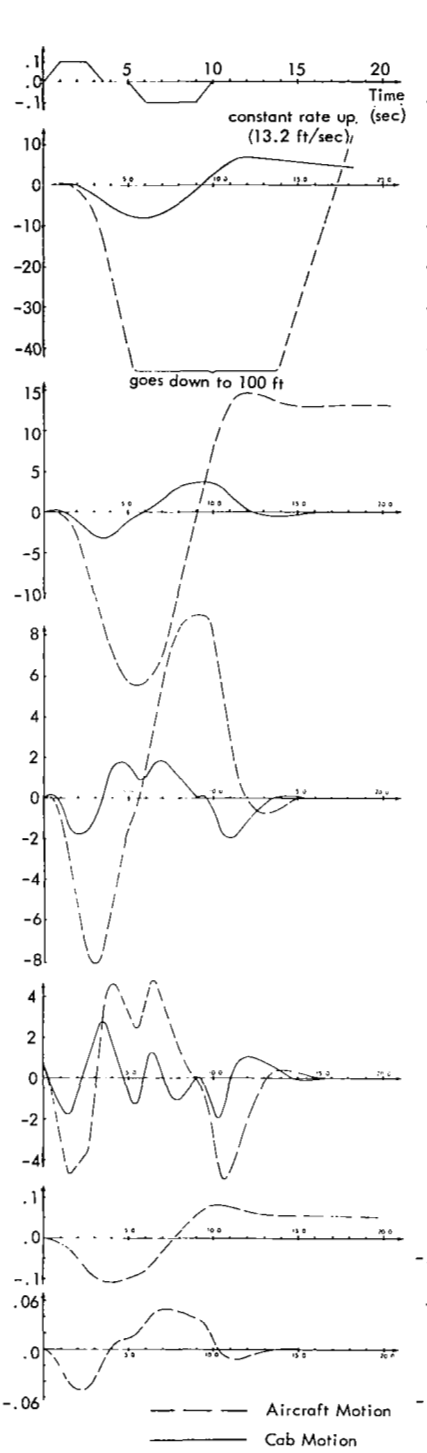

Figure 4-5
Transient Responses for Control System Using Acceleration Weighted Cost Function M_1 and Quadratic Penalty Function $L_2(\beta=1.0)$: with Double Trapezoidal Pulse Input

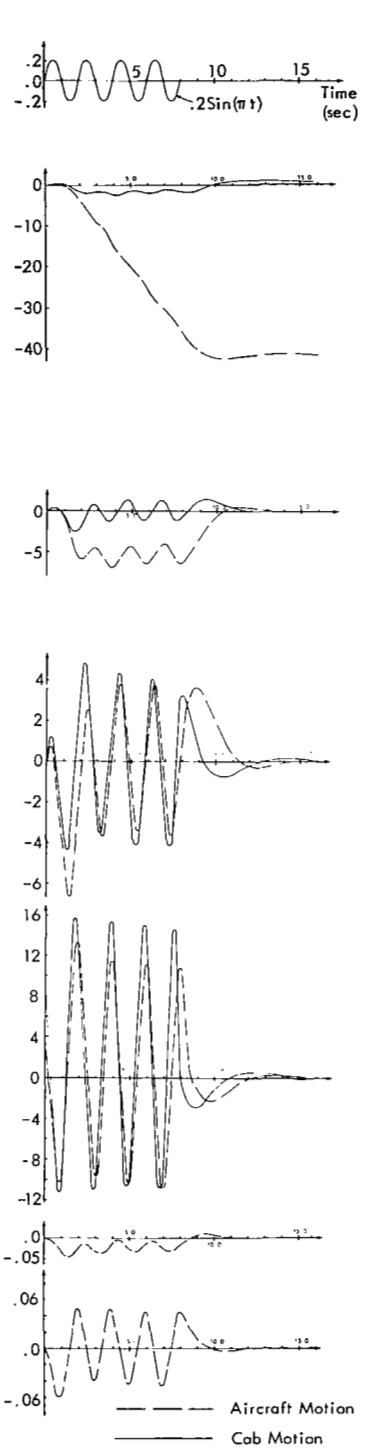

Figure 4-6
Transient Responses for Control System Using Acceleration Weighted Cost Function M_1 and Quadratic Penalty Function $L_2(\beta=1\ 0)$: with Sinusoidal Input

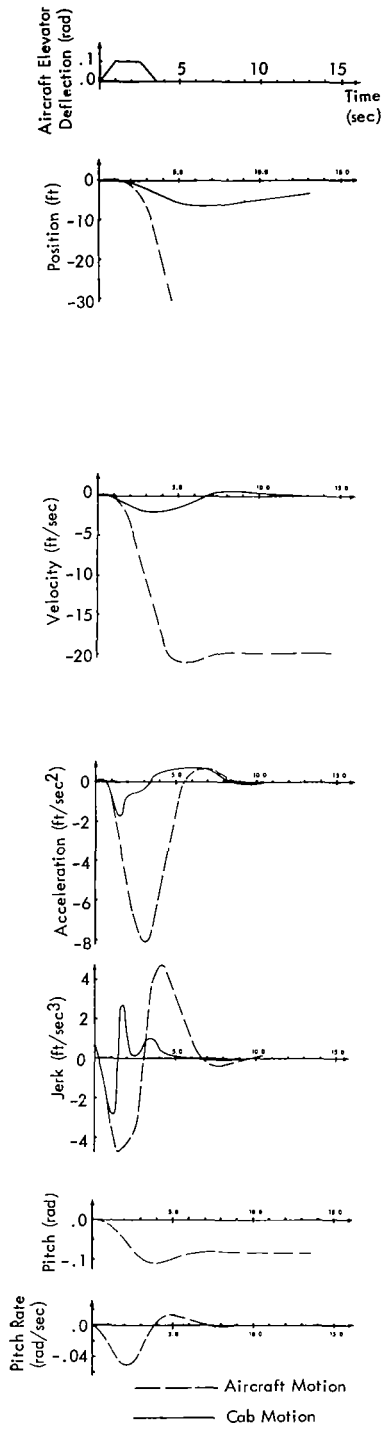

Figure 4-7
Transient Responses for Control System Using Acceleration Weighted Cost Function M_1 and Quartic Penalty Function $L_2(\beta=2.0)$: with Single Trapezoidal Pulse Input

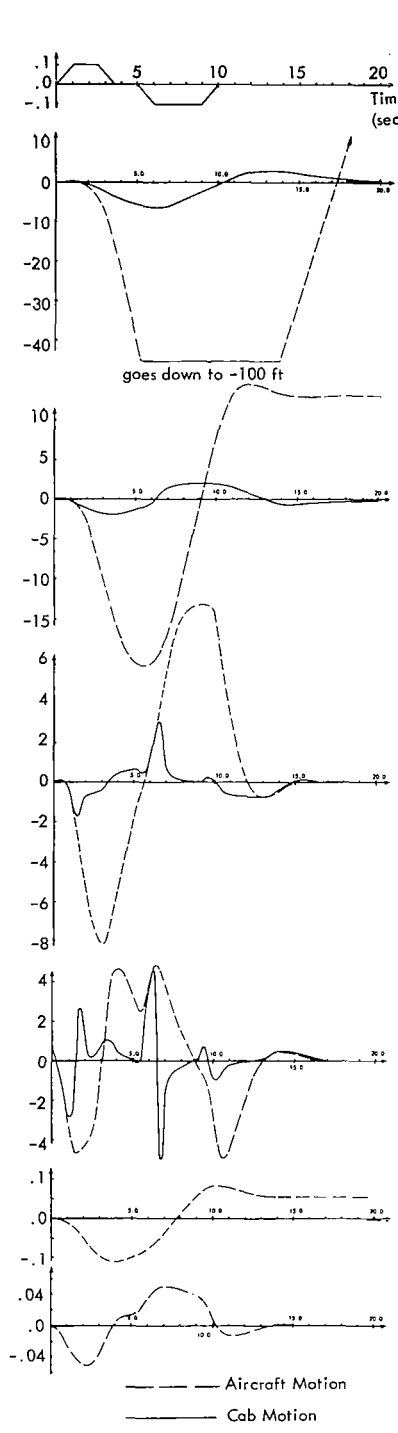

Figure 4-8
Transient Responses for Control System Using Acceleration Weighted Cost Function M_1 and Quartic Penalty Function $L_2(\beta=2.0)$: with Double Trapezoidal Pulse Input

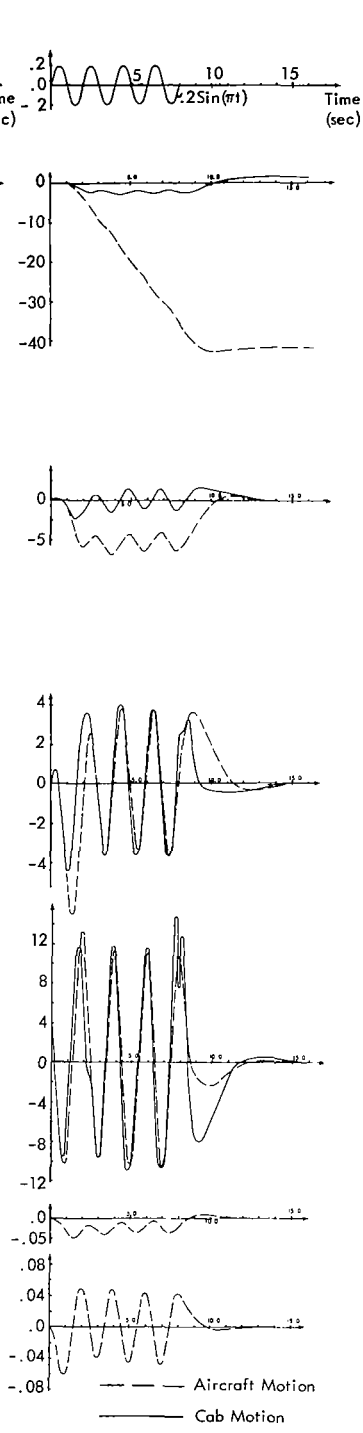

Figure 4-9
Transient Responses for Control System Using Acceleration Weighted Cost Function M_1 Quartic Penalty Function $L_2(\beta=2.0)$: with Sinusoidal Input

Table 4-2

Parameters Used in Computer Simulation of Control Scheme (M_1, L_2)

Parameters	Values Used in Figures	
	Figs. 4.4 to 4.6 $\beta = 1$	Figs. 4.7 to 4.9 $\beta = 2$
$q_{\ddot{y}}$	10.0	10.0
$q_{\dot{\theta}}$	0.0	0.0
$q_{\ddot{\theta}}$	-	-
ϵ	+0.18	+ 0.002
k	-	-
k_1	-0.1	-0.1
k_2	7.0	7.0
k_3	2.0	2.0
T	20.0	20.0
Y_c	10.0	10.0

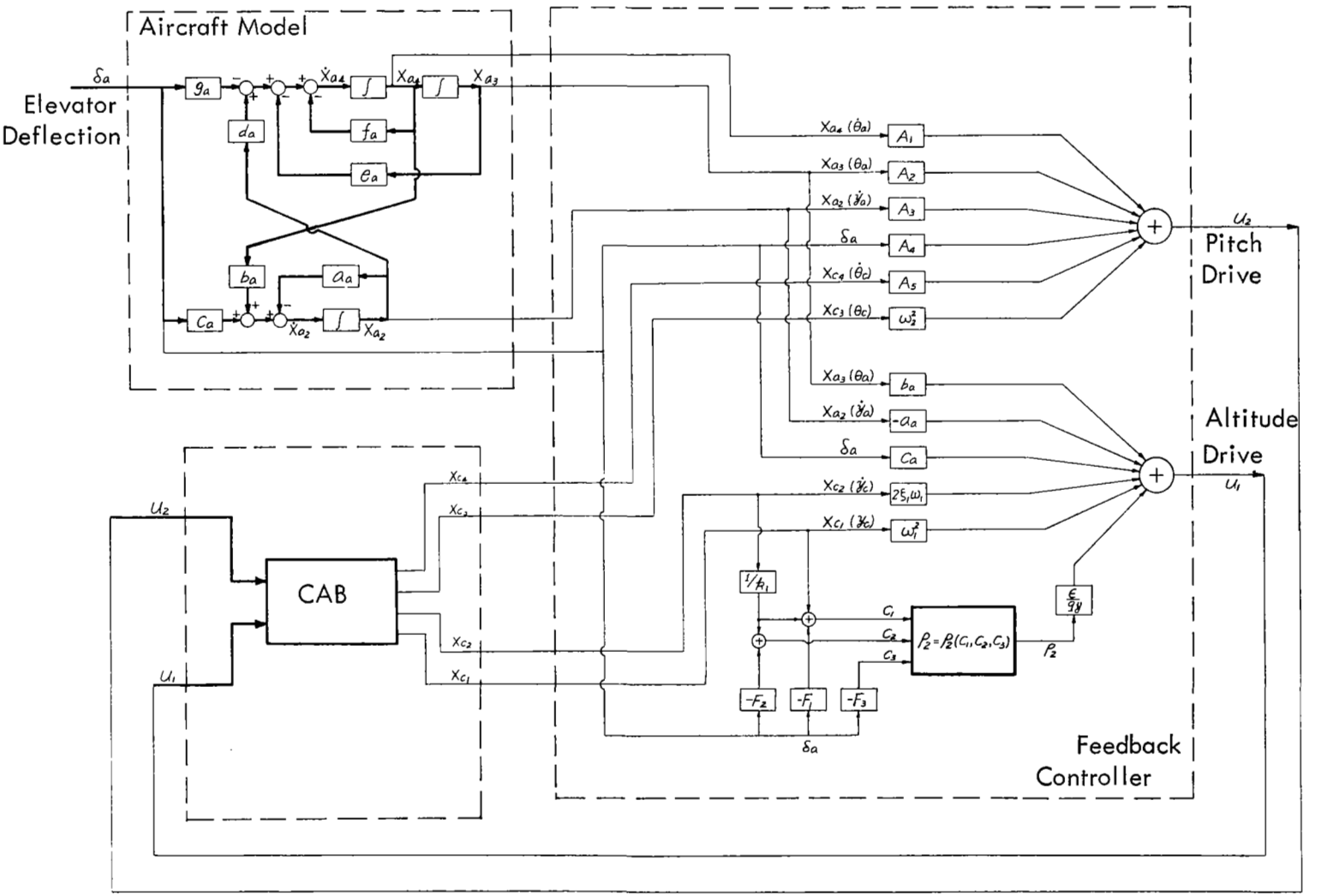

(a) component form

Fig. 4-10 Closed-Loop Realization of the Control System for the case (M_1, L_2)

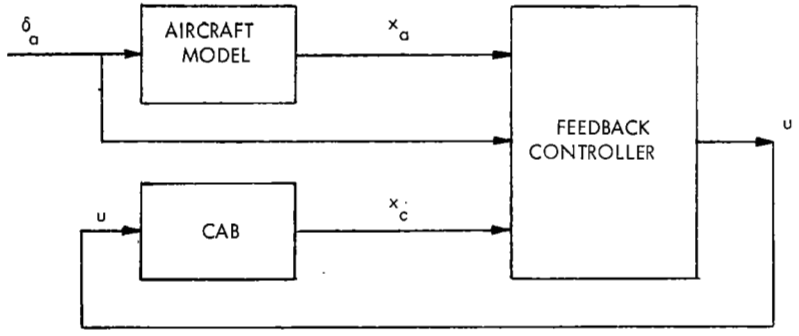

(b) vector form

Fig. 4-10 (con't)

$$A_1 = -f_a - N_{44}/q_{\ddot{\theta}}$$

$$A_2 = -e_a - N_{43}/q_{\ddot{\theta}}$$

$$A_3 = d_a - N_{42}/q_{\ddot{\theta}}$$

$$A_4 = -g_a - \frac{c_a N_{42} - g_a(\sqrt{q_{\dot{\theta}} q_{\ddot{\theta}}} + N_{44})}{k q_{\ddot{\theta}} + \sqrt{q_{\dot{\theta}} q_{\ddot{\theta}}}}$$

$$A_5 = 2\xi_2 \omega_2 - \sqrt{q_{\dot{\theta}}/q_{\ddot{\theta}}}$$

$$F_1 = \frac{k_2}{k_1 k_3}$$

$$F_2 = \frac{k_2}{k_1(k_3 - k_1)}$$

$$F_3 = \frac{k_2}{k_3(k_3 - k_1)}$$

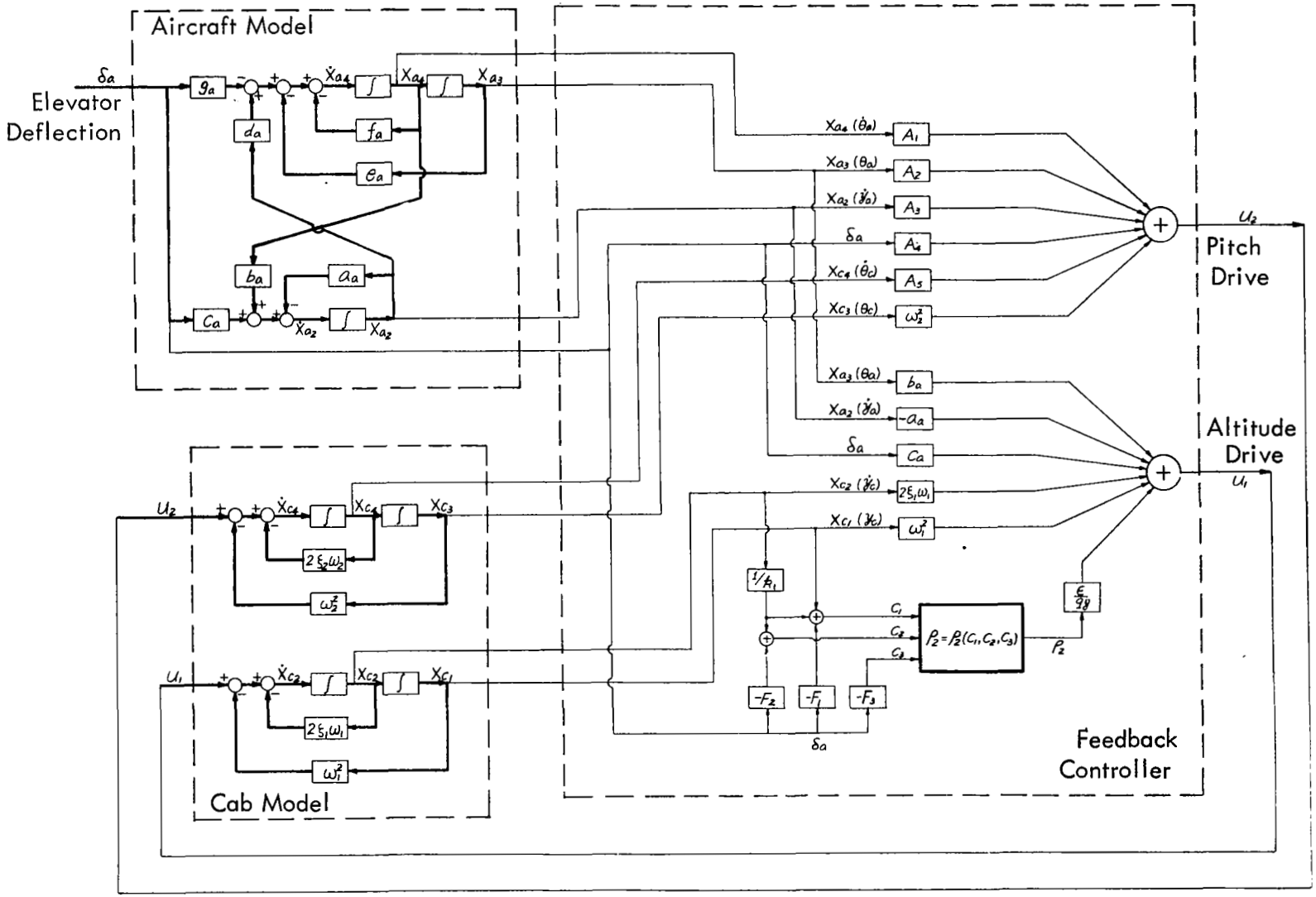

(a) component form

Fig. 4-11 Open-Loop Realization of the Control System for the case (M_1, L_2)

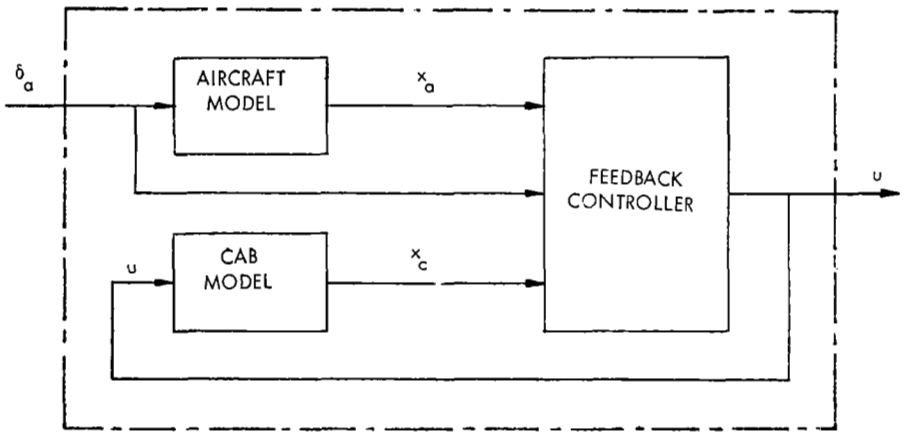

$$A_1 = -f_a - N_{44}/q_{\ddot{\theta}}$$

$$A_2 = -e_a - N_{43}/q_{\ddot{\theta}}$$

$$A_3 = d_a - N_{42}/q_{\ddot{\theta}}$$

$$A_4 = -g_a - \frac{c_a N_{42} - g_a(\sqrt{q_{\dot{\theta}} q_{\ddot{\theta}}} + N_{44})}{k q_{\ddot{\theta}} + \sqrt{q_{\dot{\theta}} q_{\ddot{\theta}}}}$$

$$A_5 = 2\xi_2 \omega_2 - \sqrt{q_{\dot{\theta}}/q_{\ddot{\theta}}}$$

$$F_1 = \frac{k_2}{k_1 k_3}$$

$$F_2 = \frac{k_2}{k_1(k_3 - k_1)}$$

$$F_3 = \frac{k_2}{k_3(k_3 - k_1)}$$

(b) vector form

Fig. 4-11 (con't)

4.3 Control System Design Using Cost Function M_2 with Jerk Weighting and "Soft" Boundary Penalty Function L_2

Although several different formulations can be conceived to include jerk error in the performance index, the following form is used since the general theory developed in Section 3 can be directly applied without any modification.

Differentiating (4.1a) and (4.2a) with respect to time τ, and let the state variables x_a, x_c be defined as follows:

$$\begin{aligned} x_{a1} &= y_a & x_{c1} &= y_c \\ x_{a2} &= \dot{y}_a & x_{c2} &= \dot{y}_c \\ x_{a3} &= \ddot{y}_a & x_{c3} &= \ddot{y}_c \\ x_{a4} &= \theta_a & x_{c4} &= \theta_c \\ x_{a5} &= \dot{\theta}_a & x_{c5} &= \dot{\theta}_c \\ x_{a6} &= \delta_a(t) & x_{c6} &= u_1 \end{aligned}$$

the dynamic equations (4.1) and (4.2) become

$$\begin{aligned} \dot{x}_{a1} &= x_{a2} \\ \dot{x}_{a2} &= x_{a3} \\ \dot{x}_{a3} &= -a_a x_{a3} + b_a x_{a5} + c_a \dot{\delta}_a \\ \dot{x}_{a4} &= x_{a5} \\ \dot{x}_{a5} &= d_a x_{a2} - e_a x_{a4} - f_a x_{a5} - g_a x_{a6} \\ \dot{x}_{a6} &= \dot{\delta}_a \end{aligned} \tag{4.39}$$

and

$$\begin{aligned} \dot{x}_{c1} &= x_{c2} \\ \dot{x}_{c2} &= x_{c3} \\ \dot{x}_{c3} &= -2\xi_1 \omega_1 x_{c3} - \omega_1^2 x_{c2} + \dot{u}_1 \\ \dot{x}_{c4} &= x_{c5} \\ \dot{x}_{c5} &= -2\xi_2 \omega_2 x_{c5} - \omega_2^2 x_{c4} + u_2 \\ \dot{x}_{c6} &= \dot{u}_1 \end{aligned} \tag{4.40}$$

and with $x = x_a - x_c$, the error dynamics are obtained from (4.39) and (4.40).

$$
\begin{aligned}
\dot{x}_1 &= x_2 \\
\dot{x}_2 &= x_3 \\
\dot{x}_3 &= \omega_1^2 x_{c2} - (a_a - 2\xi_1\omega_1)x_{c3} + b_a x_{c5} - a_a x_3 + b_a x_5 + c_a \dot{\delta}_a - \dot{u}_1 \\
\dot{x}_4 &= x_5 \\
\dot{x}_5 &= d_a x_{c2} - (e_a - \omega_2^2)x_{c4} - (f_a - 2\xi_1\omega_2)x_{c5} - g_a x_{c6} + d_a x_2 \\
&\qquad - e_a x_4 - f_a x_5 - g_a x_6 - u_2 \\
\dot{x}_6 &= \dot{\delta}_a - \dot{u}_1
\end{aligned}
\tag{4.41}
$$

Note that the control vector u and the input in this case take the form

$$
u = \begin{bmatrix} \dot{u}_1 \\ u_2 \end{bmatrix}, \quad \text{pilot input} = \dot{\delta}_a(t)
$$

and, with the cost function M_2 of (4.3), the constant weighting matrix Q is given by

$$
Q = \begin{bmatrix}
0 & 0 & 0 & 0 & 0 & 0 \\
0 & q_{\ddot{y}} & 0 & 0 & 0 & 0 \\
0 & 0 & q_{\dddot{y}} & 0 & 0 & 0 \\
0 & 0 & 0 & q_{\dot{\theta}} & 0 & 0 \\
0 & 0 & 0 & 0 & q_{\ddot{\theta}} & 0 \\
0 & 0 & 0 & 0 & 0 & 0
\end{bmatrix}
\tag{4.42}
$$

Thus, the optimal control law (3.23) becomes

$$
\begin{aligned}
\dot{u}_1 &= \omega_1^2 x_{c2} - (a_a - 2\xi_1\omega_1)x_{c3} + b_a x_{c5} - a_a x_3 + b_a x_5 + c_a \dot{\delta}_a + \frac{1}{q_{\dddot{y}}}(p_{c3} - p_3) \\
u_2 &= d_a x_{c2} - (e_a - \omega_2^2)x_{c4} - (f_a - 2\xi_2\omega_2)x_{c5} - g_a x_{c6} + d_a x_2 - e_a x_4 - f_a x_5 - g_a x_6 + \frac{1}{q_{\ddot{\theta}}}(p_{c5} - p_5)
\end{aligned}
\tag{4.43}
$$

where p, p_c are the corresponding adjoint variables as defined in Section 3. It was shown that the optimum values of $p_c - p$ can be approximated by the simplified solution $P_c - P$ and the quasi-optimum correction ρ as

$$p_c - p = P_c - P + \epsilon\rho = -N_c X_c - NX - q(t) + \epsilon\rho \tag{4.44}$$

where N_c, N and q are obtained from asymptotic solutions of (3.38), (3.39) and (3.41),

$$N = \begin{bmatrix} 0 & 0 & 0 & 0 & 0 & 0 \\ 0 & 0 & 0 & 0 & 0 & 0 \\ 0 & N_{32} & N_{33} & N_{34} & N_{35} & N_{36} \\ 0 & 0 & 0 & 0 & 0 & 0 \\ 0 & N_{52} & N_{53} & N_{54} & N_{55} & N_{56} \\ 0 & 0 & 0 & 0 & 0 & 0 \end{bmatrix} \tag{4.45}$$

$$N_c = \begin{bmatrix} 0 & 0 & 0 & 0 & 0 & 0 \\ 0 & 0 & 0 & 0 & 0 & 0 \\ 0 & N_{32} & (N_{33} + \sqrt{q_{\dot{y}} q_{\ddot{y}}}) & N_{34} & N_{35} & N_{36} \\ 0 & 0 & 0 & 0 & 0 & 0 \\ 0 & N_{52} & N_{53} & N_{54} & (N_{55} + \sqrt{q_{\dot{\theta}} q_{\ddot{\theta}}}) & N_{56} \\ 0 & 0 & 0 & 0 & 0 & 0 \end{bmatrix}$$

where:

$$N_{36} = -\frac{g_a}{\sqrt{q_{\dot{y}} / q_{\ddot{y}}}} N_{35}$$

$$N_{35} = \frac{q_{\dot{y}}}{\frac{\sqrt{q_{\dot{y}} / q_{\ddot{y}}} + a_a}{b_a}\left(\frac{e_a}{\sqrt{q_{\dot{y}} / q_{\ddot{y}}}} + \sqrt{q_{\dot{y}} / q_{\ddot{y}}} + f_a\right) - \frac{d_a}{\sqrt{q_{\dot{y}} / q_{\ddot{y}}}}}$$

$$N_{34} = -\frac{e_a}{\sqrt{q_{\dot{y}} / q_{\ddot{y}}}} N_{35}$$

$$N_{33} = \frac{1}{b_a}\left(\frac{e_a}{\sqrt{q_{\dot{y}} / q_{\ddot{y}}}} + \sqrt{q_{\dot{y}} / q_{\ddot{y}}} + f_a\right) N_{35} \tag{4.46}$$

$$N_{32} = \frac{d_a}{\sqrt{q_{\dot{y}}/q_{\ddot{y}}}} N_{35}$$

$$N_{56} = -\frac{g_a}{\sqrt{q_{\dot{\theta}}/q_{\ddot{\theta}}}} N_{55}$$

$$N_{55} = \frac{q_{\dot{\theta}}}{\sqrt{q_{\dot{\theta}}/q_{\ddot{\theta}}} + f_a + \frac{e_a}{\sqrt{q_{\dot{\theta}}/q_{\ddot{\theta}}}} - \frac{b_a d_a}{\sqrt{q_{\dot{\theta}}/q_{\ddot{\theta}}}\,(\sqrt{q_{\dot{\theta}}/q_{\ddot{\theta}}} - a_a)}}$$

$$N_{54} = -\frac{e_a}{\sqrt{q_{\dot{\theta}}/q_{\ddot{\theta}}}} N_{55}$$

$$N_{53} = \frac{d_a}{\sqrt{q_{\dot{\theta}}/q_{\ddot{\theta}}}\,(\sqrt{q_{\dot{\theta}}/q_{\ddot{\theta}}} - a_a)} N_{55}$$

$$N_{52} = \frac{d_a}{\sqrt{q_{\dot{\theta}}/q_{\ddot{\theta}}}} N_{55}$$

$$q(t) = \begin{bmatrix} 0 \\ 0 \\ q_3(t) \\ 0 \\ q_5(t) \\ 0 \end{bmatrix} \qquad (4.47)$$

$$q_3(t) = \left[c_a(N_{33} + \sqrt{q_{\dot{y}} q_{\ddot{y}}}) + N_{36} \right] \int_t^{T+t\sqrt{q_{\dot{y}}/q_{\ddot{y}}}} e^{(t-s)} \dot{\delta}_a(s)\, ds$$

$$q_5(t) = (c_a N_{53} + N_{56}) \int_t^{T+t\sqrt{q_{\dot{\theta}}/q_{\ddot{\theta}}}} e^{(t-s)} \dot{\delta}_a(s)\, ds \qquad (4.48)$$

As noted in Section 4.1, integration of (4.48) requires the knowledge of the input rate $\dot{\delta}_a$ in the future. Again using the exponential approximation

$$\dot{\delta}_a(\tau) = \delta_a(t)\, e^{-k(\tau - t)}$$

$$\delta_a(\tau) = -k\, \delta_a(t)\, e^{-k(\tau - t)} \qquad (4.49)$$

(4.48) yields

$$q_3(t) = -\frac{c_a(N_{33} + \sqrt{q_{\dot{y}} q_{\ddot{y}}}) + N_{36}}{k + \sqrt{q_{\dot{y}} q_{\ddot{y}}}} \left[e^{-(\sqrt{q_{\dot{y}}/q_{\ddot{y}}} + k)\, T} - 1 \right] \dot{\delta}_a(t)$$

$$q_5(t) = -\frac{c_a N_{53} + N_{56}}{k + \sqrt{q_{\dot{\theta}} q_{\ddot{\theta}}}} \left[e^{-(\sqrt{q_{\dot{\theta}}/q_{\ddot{\theta}}} + k)\, T} - 1 \right] \dot{\delta}_a(t) \qquad (4.50)$$

As $T \to \infty$ (4.50) further reduces to

$$q_3 = \frac{c_a(N_{33} + \sqrt{q_{\dot{y}} q_{\ddot{y}}}) + N_{36}}{k + \sqrt{q_{\dot{y}}/q_{\ddot{y}}}} \dot{\delta}_a$$

$$q_5 = \frac{c_a N_{53} + N_{56}}{k + \sqrt{q_{\dot{\theta}}/q_{\ddot{\theta}}}} \dot{\delta}_a \qquad (4.51)$$

Thus, from (4.43) and (4.44), the simplified control $\dot{U}_1$ and U_2, with $\epsilon = 0$, are written as

$$\dot{U}_1 = (\omega_1^2 - \frac{N_{32}}{q_{\dddot{y}}}) X_{c2} + (2\xi_1\omega_1 - a_a - \frac{N_{33} + \sqrt{q_{\dot{y}} q_{\dddot{y}}}}{q_{\dddot{y}}}) X_{c3} - \frac{N_{34}}{q_{\dddot{y}}} X_{c4} + (b_a - \frac{N_{35}}{q_{\dddot{y}}}) X_{c5}$$

$$- \frac{N_{36}}{q_{\dddot{y}}} X_{c6} - \frac{N_{32}}{q_{\dddot{y}}} X_2 - (a_a + \frac{N_{33}}{q_{\dddot{y}}}) X_3 - \frac{N_{34}}{q_{\dddot{y}}} X_4 + (b_a - \frac{N_{35}}{q_{\dddot{y}}}) X_5 - \frac{N_{36}}{q_{\dddot{y}}} X_6$$

$$+ c_a \dot{\delta}_a - \frac{q_3}{q_{\dddot{y}}} \qquad (4.52)$$

$$U_2 = (d_a - \frac{N_{52}}{q_{\ddot{\theta}}}) X_{c2} - \frac{N_{53}}{q_{\ddot{\theta}}} X_{c3} + (\omega^2 - e_a - \frac{N_{54}}{q_{\ddot{\theta}}}) X_{c4} + (2\xi_2\omega_2 - f_a - \frac{N_{55} + \sqrt{q_{\dot{\theta}} q_{\ddot{\theta}}}}{q_{\ddot{\theta}}}) X_{c5}$$

$$- (g_a + \frac{N_{56}}{q_{\ddot{\theta}}}) X_{c6} + (d_a - \frac{N_{52}}{q_{\ddot{\theta}}}) X_2 - \frac{N_{53}}{q_{\ddot{\theta}}} X_3 - (e_a + \frac{N_{54}}{q_{\ddot{\theta}}}) X_4$$

$$- (f_a + \frac{N_{55}}{q_{\ddot{\theta}}}) X_5 - (g_a + \frac{N_{56}}{q_{\ddot{\theta}}}) X_6 - \frac{q_5}{q_{\ddot{\theta}}}$$

Substitution of (4.52) into (4.40), and using the relation $X = x_a - X_c$ to eliminate the error state X, we obtain the closed-loop "simplified" system equations for the cab,

$$\dot{X}_{c1} = X_{c2}$$

$$\dot{X}_{c2} = X_{c3}$$

$$\dot{X}_{c3} = -\sqrt{q_{\dot{y}}/q_{\dddot{y}}}\, X_{c3} - \frac{N_{32}}{q_{\dddot{y}}} x_{a2} - (a_a + \frac{N_{33}}{q_{\dddot{y}}}) x_{a3} - \frac{N_{34}}{q_{\dddot{y}}} x_{a4} + (b_a - \frac{N_{35}}{q_{\dddot{y}}}) x_{a5}$$

$$- \frac{N_{36}}{q_{\dddot{y}}} x_{a6} + c_a \dot{\delta}_a - \frac{q_3}{q_{\dddot{y}}} \qquad (4.53)$$

$$\dot{X}_{c4} = X_{c5}$$

$$\dot{X}_{c5} = -\sqrt{q_{\dot{\theta}}/q_{\ddot{\theta}}}\, X_{c5} + (d_a - \frac{N_{52}}{q_{\ddot{\theta}}}) x_{a2} - \frac{N_{53}}{q_{\ddot{\theta}}} x_{a3} - (e_a + \frac{N_{54}}{q_{\ddot{\theta}}}) x_{a4}$$

$$- (f_a + \frac{N_{55}}{q_{\ddot{\theta}}}) x_{a5} - (g_a + \frac{N_{56}}{q_{\ddot{\theta}}}) x_{a6} - \frac{q_5}{q_{\ddot{\theta}}}$$

$$\dot{X}_{c6} = \dot{U}_1$$

Or, in view of the aircraft dynamics (4.39), (4.53) can be rewritten as

$$
\begin{aligned}
\dot{X}_{c1} &= X_{c2} \\
\dot{X}_{c2} &= X_{c3} \\
\dot{X}_{c3} &= \dot{x}_{a3} - \sqrt{q_{\dddot{y}}/q_{\ddot{y}}}\, X_{c3} - \frac{N_{32}}{q_{\ddot{y}}} x_{a2} - \frac{N_{33}}{q_{\ddot{y}}} x_{a3} - \frac{N_{34}}{q_{\ddot{y}}} x_{a4} \\
&\quad - \frac{N_{35}}{q_{\ddot{y}}} x_{a5} - \frac{N_{36}}{q_{\ddot{y}}} x_{a6} - \frac{q_3}{q_{\ddot{y}}} \\
\dot{X}_{c4} &= X_{c5} \\
\dot{X}_{c5} &= \dot{x}_{a5} - \sqrt{q_{\dot{\theta}}/q_{\ddot{\theta}}}\, X_{c5} - \frac{N_{52}}{q_{\ddot{\theta}}} x_{a2} - \frac{N_{53}}{q_{\ddot{\theta}}} x_{a3} - \frac{N_{54}}{q_{\ddot{\theta}}} x_{a4} \\
&\quad - \frac{N_{55}}{q_{\ddot{\theta}}} x_{a5} - \frac{N_{56}}{q_{\ddot{\theta}}} x_{a6} - \frac{q_5}{q_{\ddot{\theta}}} \\
\dot{X}_{c6} &= \dot{U}_1
\end{aligned}
\tag{4.54}
$$

It can be seen from (4.46) and (4.48) that the weighting coefficients $q_{\ddot{y}}$ and $q_{\dddot{y}}$ appear in the terms $\frac{N_{32}}{q_{\dddot{y}}}$, $\frac{N_{33}}{q_{\dddot{y}}}$, $\frac{N_{34}}{q_{\dddot{y}}}$, $\frac{N_{35}}{q_{\dddot{y}}}$, $\frac{N_{36}}{q_{\dddot{y}}}$, $\frac{q_3}{q_{\dddot{y}}}$ only in the form of $q_{\ddot{y}}/q_{\dddot{y}}$ and that all these terms can be made to any small value by letting $q_{\ddot{y}}/q_{\dddot{y}} \to 0$. Similarly, the terms $\frac{N_{52}}{q_{\ddot{\theta}}}$, $\frac{N_{53}}{q_{\ddot{\theta}}}$, $\frac{N_{54}}{q_{\ddot{\theta}}}$, $\frac{N_{55}}{q_{\ddot{\theta}}}$, $\frac{N_{56}}{q_{\ddot{\theta}}}$, $\frac{q_5}{q_{\ddot{\theta}}}$ depend solely on the ratio $q_{\dot{\theta}}/q_{\ddot{\theta}}$ and can all be made to any small value desired by letting $q_{\dot{\theta}}/q_{\ddot{\theta}}$ be small. Thus, it is clear from the closed-loop simplified system (4.54) that the simplified control essentially cancels out the original cab dynamics and substitutes in its place a dynamics that can be made close to that of aircraft dynamics by adjusting the two ratios $q_{\ddot{y}}/q_{\dddot{y}}$ and $q_{\dot{\theta}}/q_{\ddot{\theta}}$. It would appear, intuitively, that since there is no constraint on the angular motion (X_{c4}, X_{c5}), the ratio $q_{\dot{\theta}}/q_{\ddot{\theta}}$ can be chosen to be 0 so that the angular motion of the cab duplicates that of the aircraft exactly.

The quasi-optimum correction factor ρ is obtained by solving (3.56) which in the present case becomes

$$
\begin{aligned}
\dot{\rho}_1 &= \frac{\partial L}{\partial X_{c1}} \\
\dot{\rho}_2 &= -\rho_1 - \omega_1^2 \rho_6 \\
\dot{\rho}_3 &= -\rho_2 + \sqrt{q_{\dot{y}}/q_{\dddot{y}}}\ \rho_3 - (2\xi_1 \omega_1 - \sqrt{q_{\dot{y}}/q_{\dddot{y}}})\ \rho_6 \\
\dot{\rho}_4 &= 0 \\
\dot{\rho}_5 &= -\rho_4 + \sqrt{q_{\dot{\theta}}/q_{\ddot{\theta}}}\ \rho_5 \\
\dot{\rho}_6 &= 0
\end{aligned}
\tag{4.55}
$$

with $\rho(T) = 0$.

Obviously, (4.55) gives $\rho_4 = \rho_5 = \rho_6 \equiv 0$, which is well expected since, as noted in the beginning of Section 4, no limitation was imposed on, and, therefore, no washout would be necessary for the angular motion. Hence

$$
\rho(t) = \begin{bmatrix} \rho_1(t) \\ \rho_2(t) \\ \rho_3(t) \\ 0 \\ 0 \\ 0 \end{bmatrix} \tag{4.56}
$$

Thus, the quasi-optimum control law is obtained by substituting (4.56) and (4.44) into (4.43),

$$\dot{v}_1 \simeq (\omega_1^2 - \frac{N_{32}}{q_{\dddot{y}}}) x_{c2} + (2\xi_1 \omega_1 - a_a - \frac{N_{33} + \sqrt{q_{\dot{y}} q_{\dddot{y}}}}{q_{\dddot{y}}}) x_{c3} - \frac{N_{34}}{q_{\dddot{y}}} x_{c4} + (b_a - \frac{N_{35}}{q_{\dddot{y}}}) x_{c5}$$

$$- \frac{N_{36}}{q_{\dddot{y}}} x_{c6} - \frac{N_{32}}{q_{\dddot{y}}} x_2 - (a_a + \frac{N_{33}}{q_{\dddot{y}}}) x_3 - \frac{N_{34}}{q_{\dddot{y}}} x_4 + (b_a - \frac{N_{35}}{q_{\dddot{y}}}) x_5 - \frac{N_{36}}{q_{\dddot{y}}} x_6$$

$$+ c_a \dot{\delta}_a - \frac{q_3}{q_{\dddot{y}}} + \frac{\epsilon}{q_{\dddot{y}}} \rho_3$$

(4.57)

$$v_2 \simeq (d_a - \frac{N_{52}}{q_{\ddot{\theta}}}) x_{c2} - \frac{N_{53}}{q_{\ddot{\theta}}} x_{c3} + (\omega_2^2 - e_a - \frac{N_{54}}{q_{\ddot{\theta}}}) x_{c4} + (2\xi_2 \omega_2 - f_a - \frac{N_{55} + \sqrt{q_{\dot{\theta}} q_{\ddot{\theta}}}}{q_{\ddot{\theta}}}) x_{c5}$$

$$- (g_a + \frac{N_{56}}{q_{\ddot{\theta}}}) x_{c6} + (d_a - \frac{N_{52}}{q_{\ddot{\theta}}}) x_2 - \frac{N_{53}}{q_{\ddot{\theta}}} x_3 - (e_a + \frac{N_{54}}{q_{\ddot{\theta}}}) x_4$$

$$- (f_a + \frac{N_{55}}{q_{\ddot{\theta}}}) x_5 - (g_a + \frac{N_{56}}{q_{\ddot{\theta}}}) x_6 - \frac{q_5}{q_{\ddot{\theta}}}$$

or, using $x + x_c = x_a$, (4.57) is rewritten as

$$\dot{v}_1 \simeq \omega_1^2 x_{c2} + (2\xi_1 \omega_1 - \sqrt{q_{\dot{y}} / q_{\dddot{y}}}) x_{c3} - \frac{N_{32}}{q_{\dddot{y}}} x_{a2} - (a_a + \frac{N_{33}}{q_{\dddot{y}}}) x_{a3}$$

$$- \frac{N_{34}}{q_{\dddot{y}}} x_{a4} + (b_a - \frac{N_{35}}{q_{\dddot{y}}}) x_{a5} - \frac{N_{36}}{q_{\dddot{y}}} x_{a6} + c_a \dot{\delta}_a - \frac{q_3}{q_{\dddot{y}}} + \frac{\epsilon}{q_{\dddot{y}}} \rho_3$$

(4.58)

$$v_2 \simeq \omega_2^2 x_{c4} + (2\xi_2 \omega_2 - \sqrt{q_{\dot{\theta}} / q_{\ddot{\theta}}}) x_{c5} + (d_a - \frac{N_{52}}{q_{\ddot{\theta}}}) x_{a2} - \frac{N_{53}}{q_{\ddot{\theta}}} x_{a3}$$

$$- (e_a + \frac{N_{54}}{q_{\ddot{\theta}}}) x_{a4} - (f_a + \frac{N_{55}}{q_{\ddot{\theta}}}) x_{a5} - (g_a + \frac{N_{56}}{q_{\ddot{\theta}}}) x_{a6} - \frac{q_5}{q_{\ddot{\theta}}}$$

Substitution of the quasi-optimum control law (4.58) into the cab dynamics (4.40) results in closed-loop quasi-optimum system equations,

$$\dot{x}_{c1} = x_{c2}$$

$$\dot{x}_{c2} = x_{c3}$$

$$\dot{x}_{c3} = \dot{x}_{a3} - \sqrt{q_{\dddot{y}}/q_{\dddot{y}}}\, x_{c3} - \frac{N_{32}}{q_{\dddot{y}}} x_{a2} - \frac{N_{33}}{q_{\dddot{y}}} x_{a3} - \frac{N_{34}}{q_{\dddot{y}}} x_{a4}$$
$$- \frac{N_{35}}{q_{\dddot{y}}} x_{a5} - \frac{N_{36}}{q_{\dddot{y}}} x_{a6} - \frac{q_3}{q_{\dddot{y}}} + \frac{\epsilon}{q_{\dddot{y}}} \rho_3 \qquad (4.59)$$

$$\dot{x}_{c4} = x_{c5}$$

$$\dot{x}_{c5} = \dot{x}_{a5} - \sqrt{q_{\dddot{\theta}}/q_{\dddot{\theta}}}\, x_{c5} - \frac{N_{52}}{q_{\dddot{\theta}}} x_{a2} - \frac{N_{53}}{q_{\dddot{\theta}}} x_{a3} - \frac{N_{54}}{q_{\dddot{\theta}}} x_{a4}$$
$$- \frac{N_{55}}{q_{\dddot{\theta}}} x_{a5} - \frac{N_{56}}{q_{\dddot{\theta}}} x_{a6} - \frac{q_5}{q_{\dddot{\theta}}}$$

$$\dot{x}_{c6} = \dot{u}_1$$

The system equation (4.59) together with the aircraft dynamics (4.39) will be used extensively in the subsequent computer simulation study on the effect of the quasi-optimum wash-out ρ_3.

The washout ρ_3 is calculated as follows:

Calculation of ρ_3 - For

$$L_2(X_c) = \left(\frac{X_{c1}}{Y_c}\right)^{2\beta} \qquad \beta \geq 1 \qquad (4.60)$$

and

$$\frac{\partial L_2}{\partial X_{c1}} = \frac{2\beta}{Y_c^{2\beta}} X_{c1}^{(2\beta-1)}$$

it was noted in the preceding section that the main difficulty of solving ρ_3 from (4.55) with the "forcing" term given by (4.60) is the necessity of first solving X_{c1} from the closed-loop simplified system (4.53) and (4.39). Obviously, many approximation schemes can be conceived to obtain X_{c1} in sufficiently simple forms so that subsequent integration of (4.55) can be facilitated. After several trials, and with the experience accumulated up to this point, we used the following argument to achieve the desired simplification.

It is observed that since, in this design procedure, the parameters $q_{\dddot{y}}$, $q_{\ddot{y}}$, $q_{\dot{\theta}}$, $q_{\ddot{\theta}}$ are to be so adjusted that the simplified system approximately duplicates the motion of the aircraft, we should have at any instant τ,

$$\dddot{X}_{c1}(\tau) \simeq \ddot{x}_{a1}(\tau)$$

Again, using the exponential approximation of the $\ddot{x}_{a1}$, we let $\dddot{X}_{c1}$ be governed by

$$\dddot{X}_{c1}(\tau) + k_1 \ddot{X}_{c1}(\tau) = k_2 \dot{x}_{a3} e^{-k_3(\tau - t)} \tag{4.61}$$

where k_1, k_2, k_3 are to be chosen empirically, $t \le \tau \le T + t$ and $\dot{x}_{a3} \triangleq \dddot{x}_{a1}$

Assuming that the present time $t = 0$, the solution if (4.61) results in

$$X_{c1}(\tau) = C_1 + C_2\tau + C_3 e^{-k_1\tau} + C_4 e^{-k_3\tau} \tag{4.62}$$

where

$$C_1 = X_{c1} - \frac{X_{c3}}{k_1^2} - \frac{k_2(k_1 + k_3)}{k_1^2 k_3^2} \dot{x}_{a3}$$

$$C_2 = X_{c2} + \frac{X_{c3}}{k_1} + \frac{k_2}{k_1 k_3}\,\dot{x}_{a3}$$

$$C_3 = \frac{X_{c3}}{k_1^2} - \frac{k_2}{k_1^2(k_1 - k_3)}\,\dot{x}_{a3} \qquad (4.63)$$

$$C_4 = \frac{k_2}{k_3^2(k_1 - k_3)}\,\dot{x}_{a3}$$

$$\dot{x}_{a3} = -a_a x_{a3} + b_a x_{a5} + C_a \dot{\delta}_a$$

Thus, substitution of (4.62) into (4.59) and subsequently into (4.55) yields:

For $\beta = 1$,

$$\rho_3 = \frac{2}{Y_c^2}\,(D_1 C_1 + D_2 C_2 + D_3 C_3 + D_4 C_4) \qquad (4.64)$$

where

$$D_1 = \frac{1}{q_{23}^3}\left(-\frac{q_{23}^2}{2}\,T^2 + q_{23}\,T - 1 + e^{-q_{23}T}\right)$$

$$D_2 = \frac{1}{q_{23}^4}\left[-\frac{q_{23}^3}{3}\,T^3 + \frac{q_{23}^2}{2}\,T^2 - 1 + (q_{23}\,T + 1)\,e^{-q_{23}T}\right] \qquad (4.65)$$

$$D_3 = \frac{1}{q_{23}^2 k_1^2 (q_{23} + k_1)}\left\{\left[k_1 q_{23}(k_1 + q_{23})\,T + k_1^2\left(e^{-q_{23}T} - 1\right)\right]\,e^{-k_1 T} + q_{23}^2\left(e^{-k_1 T} - 1\right)\right\}$$

$$D_4 = \frac{1}{q_{23}^2 k_3^2 (q_{23} + k_3)}\left\{\left[k_3 q_{23}(k_3 + q_{23})\,T + k_3^2\left(e^{-q_{23}T} - 1\right)\right]\,e^{-k_3 T} + q_{23}^2\left(e^{-k_3 T} - 1\right)\right\}$$

$$q_{23} = \sqrt{q_{\dot{y}\dot{y}}/q_{\ddot{y}\ddot{y}}}$$

T = empirically chosen value of terminal time.

Typical trajectories generated by the control (4.58) with "washout" ρ_3, (4.64) are shown in Figures 4-12, 4-13 and 4-14 for values listed in Table 4-3 of the parameters $q_{\dot{y}}$, $q_{\dddot{y}}$, $q_{\dot{\theta}}$, $q_{\ddot{\theta}}$, ϵ, k, k_1, k_2, k_3, T and Y_c. In these figures, the cab motions are drawn in solid lines, while the corresponding aircraft motions are represented by dashed lines. Note that the weighting coefficient $q_{\dot{\theta}}$ has been set to 0 so that the angular motion of the cab becomes identical to that of aircraft's (refer to the comment following equation (4.54)). Therefore, only the aircraft's angular motion (pitch and pitch rate) is shown in the figures.

The procedure followed in adjusting the parameters was: first select a set of ($q_{\dot{y}}$, $q_{\dddot{y}}$, $q_{\dot{\theta}}$, $q_{\ddot{\theta}}$, k) so that the motion of simplified system approximates that of aircraft motion, then adjust (ϵ, T, Y_c, k_1, k_2, k_3) to obtain good acceleration and jerk profile for the quasi-optimum cab motion, and finally readjust ($q_{\dddot{y}}$, k_2, ϵ) to confine cab displacement within boundary.

It is seen from Figures 4-12, 4-13 and 4-14 that the acceleration and jerk profiles in this case show excellent phase relations between the cab and aircraft motions as compared to the previous cases in which jerk weighting was not used. The improvements in the phase relations, however, also result in deteriorated "onset" and attenuation of the general magnitudes of the accelerations. Examination of the numerical values Table 4-3 used in generating these trajectories and the structure of the washout ρ_3 in (4.64) indicates that the washout is dominated by the term $\dot{x}_{a3}$. Thus it would appear that a nonlinear washout with $\beta > 1$ in (4.58) could provide the desired compromise between phase, "onset" and magnitude relations.

An exact derivation of ρ_3 with $\beta > 1$ is rather complicated. Thus, in order to see the possible effect of nonlinear washout we simply let

$$\rho_3 = - (\dot{x}_{a3})^{(2\beta - 1)} \tag{4.66}$$

For $\beta = 1.25$, the resulting trajectories are shown in Fig. 4-15. It is apparent from the figure that the phase and "onset" relations for this case show further improvements over that of the preceding case, for which the washout takes a linear form, but the magnitude relations for the acceleration and the jerk appear somewhat irregular. The numerical data for the adjustable parameters in this case is tabulated in the second column of Table 4-2.

It should be noted that, strictly speaking, (4.66) is not a valid approximation, since it does not provide acceptable trajectories for pilot's input other than that shown in Figure 4-15. However, it does provide an evidence that a reasonable compromise among the pertinent factors governing the realism of motion simulation can be achieved by a nonlinear washout that may result from a proper choice of β . A complete block diagram of the implementation of the control law by means of an analog computer is shown in Figure 4-16 for closed-loop control and in Figure 4-17 for an open-loop control. *

*It has been subsequently established that due to a numerical integration inaccuracy, the results on page 70 are slightly in error while those on page 71 are somewhat more in error. Fortunately the shapes of the jerk and acceleration curves, which are of greatest importance in motion sensing, are close to those given but the velocities do not go to zero as is required in order for the cab displacement to reach a constant value. Thus further adjustment of the free parameters would be required to satisfy this requirement.

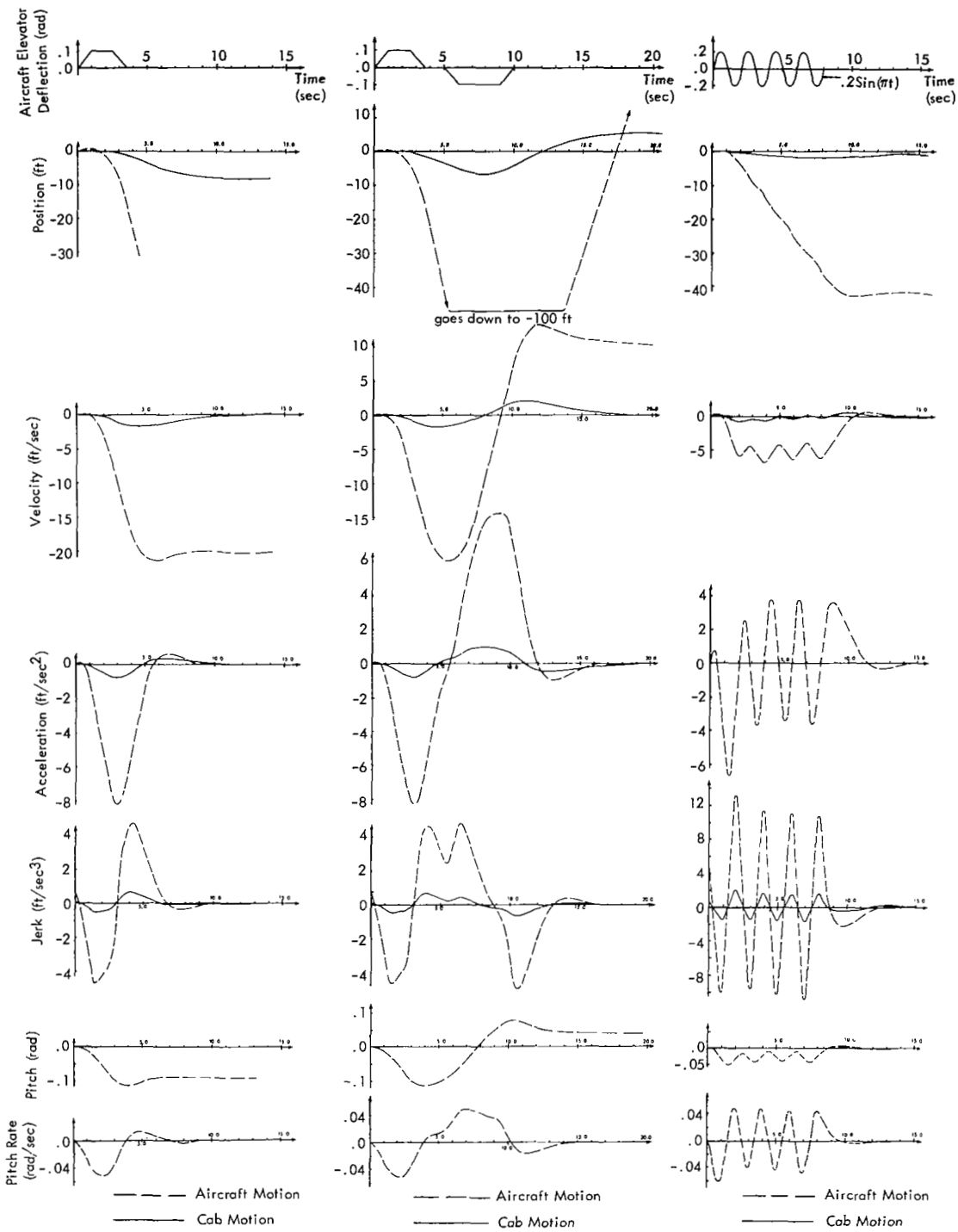

Figure 4-12
Transient Responses for Control System Using Acceleration and Jerk Weighted Cost Function M_2 and Quadratic Penalty Function $L_2(\beta=1.0)$: with Single Trapezoidal Pulse Input

Figure 4-13
Transient Responses for Control System Using Acceleration and Jerk Weighted Cost Function M_2 and Quadratic Penalty Function $L_2(\beta=1.0)$: with Double Trapezoidal Pulse Input

Figure 4-14
Transient Responses for Control System Using Acceleration and Jerk Weighted Cost Function M_2 and Quadratic Penalty Function $L_2(\beta=1.0)$: with Sinusoidal Input

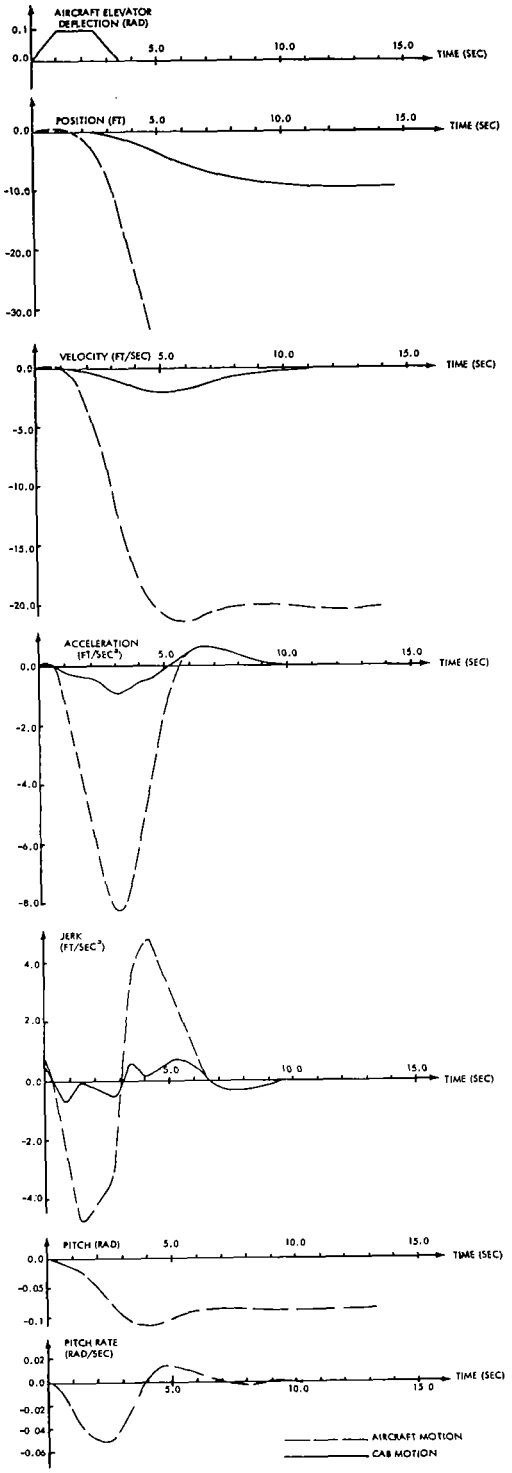

FIGURE 4-15

TRANSIENT RESPONSES FOR CONTROL SYSTEM USING ACCELERATION AND JERK WEIGHTED COST FUNCTION M_2 AND 2.5 POWER PENALTY FUNCTION $L_2(\beta=1.25)$: WITH SINGLE TRAPEZOIDAL PULSE INPUT

Table 4-3

Parameters Used in Computer Simulation of Control Scheme (M_2 , L_2)

Parameters	Values Used in Figures	
	Figs. 4.12 to 4.14 $\beta = 1.0$	Fig. 4.15 $\beta = 1.25$
$q_{\ddot{y}}$	1.0	1.0
$q_{\dddot{y}}$	5000	8000
$q_{\dot{\theta}}$	0.0	0.0
$q_{\ddot{\theta}}$	-	-
ϵ	0.3	3592.0
k	1000.0	3.0
k_1	0.1	-
k_2	7.0	-
k_3	2.0	-
T	100.0	-
Y_c	200.0	-

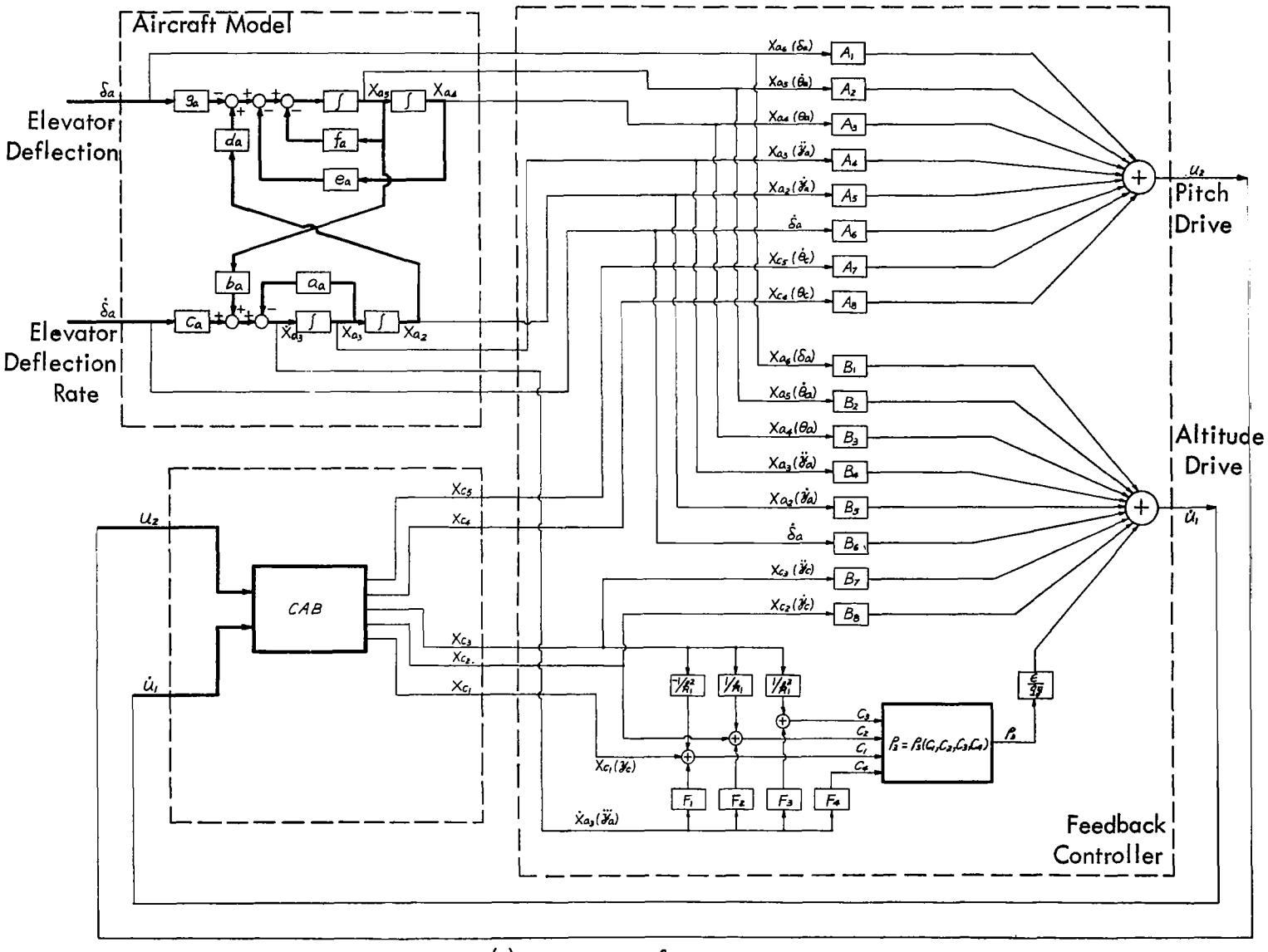

(a) component form

Fig. 4-16 Closed-Loop Realization of the Control System for the case (M_2, L_2)

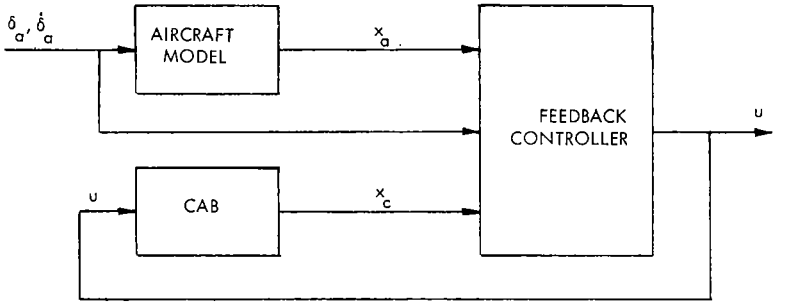

(b) vector form

Fig. 4-16 (con't)

$$A_1 = -g_a - N_{56}/q_{\ddot{\theta}}$$

$$A_2 = -f_a - N_{55}/q_{\ddot{\theta}}$$

$$A_3 = -e_a - N_{54}/q_{\ddot{\theta}}$$

$$A_4 = -N_{53}/q_{\ddot{\theta}}$$

$$A_5 = d_a - N_{52}/q_{\ddot{\theta}}$$

$$A_6 = -\frac{c_a N_{53} + N_{56}}{k q_{\ddot{\theta}} + \sqrt{q_{\dot{\theta}} q_{\ddot{\theta}}}}$$

$$A_7 = 2\xi_2\omega_2 - \sqrt{q_{\dot{\theta}}/q_{\ddot{\theta}}}$$

$$A_8 = \omega_2^2$$

$$B_1 = -N_{36}/q_{\dddot{y}}$$

$$B_2 = b_a - N_{35}/q_{\dddot{y}}$$

$$B_3 = -N_{34}/q_{\dddot{y}}$$

$$B_4 = -a_a - N_{33}/q_{\dddot{y}}$$

$$B_5 = -N_{32}/q_{\dddot{y}}$$

$$B_6 = c_a - \frac{c_a(N_{33} + \sqrt{q_{\dot{y}} q_{\dddot{y}}}) + N_{36}}{k q_{\dddot{y}} + \sqrt{q_{\dot{y}} q_{\dddot{y}}}}$$

$$B_7 = 2\xi_1\omega_1 - \sqrt{q_{\dot{y}}/q_{\dddot{y}}}$$

$$B_8 = \omega_1^2$$

$$F_1 = -\frac{k_2(k_1 + k_3)}{k_1^2 k_3^2}$$

$$F_2 = \frac{k_2}{k_1 k_3}$$

$$F_3 = -\frac{k_2}{k_1^2(k_1 - k_3)}$$

$$F_4 = \frac{k_2}{k_3^2(k_1 - k_3)}$$

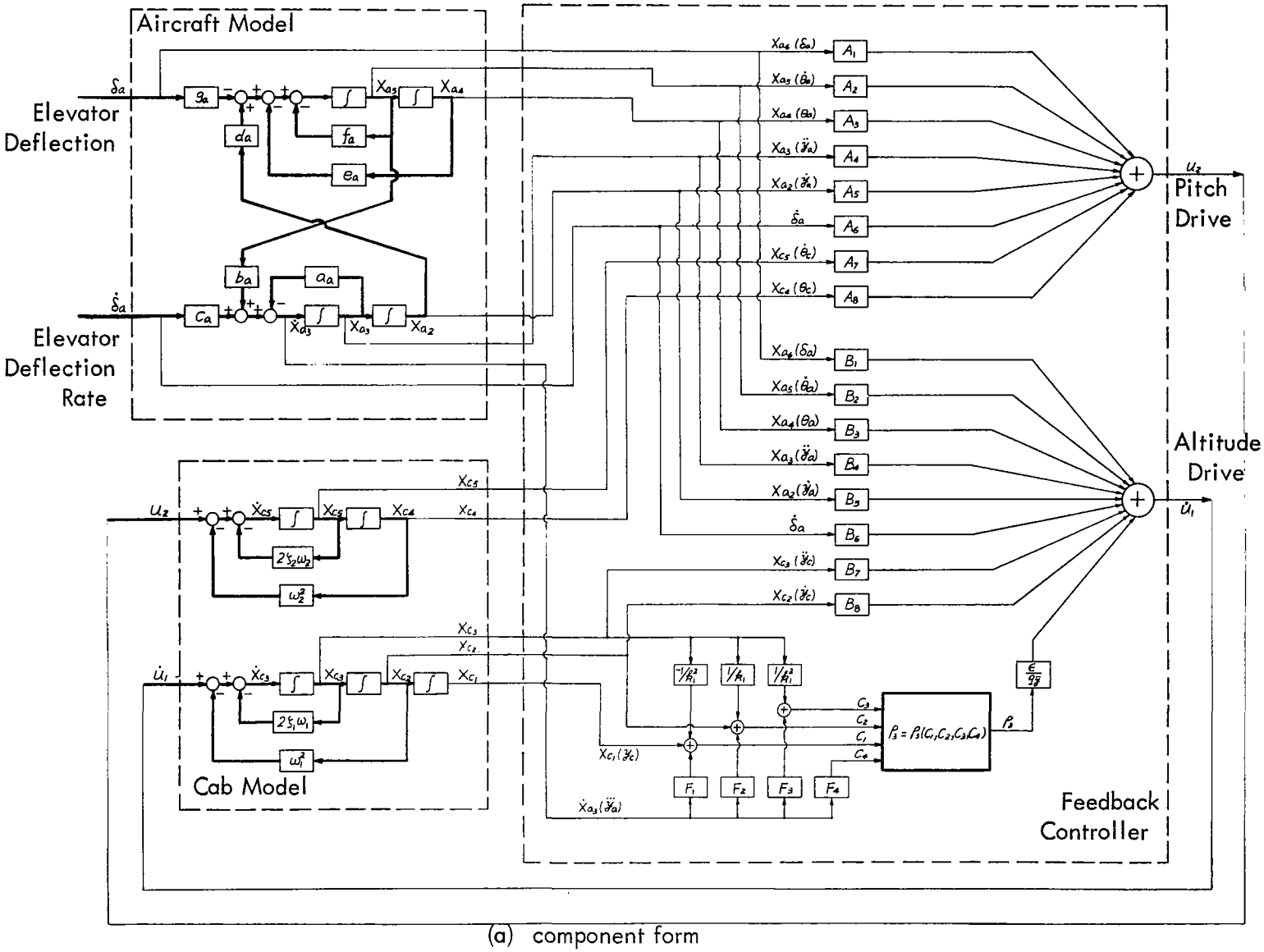

(a) component form

Fig. 4-17 Open-Loop Realization of the Control System for the case (M_2, L_2)

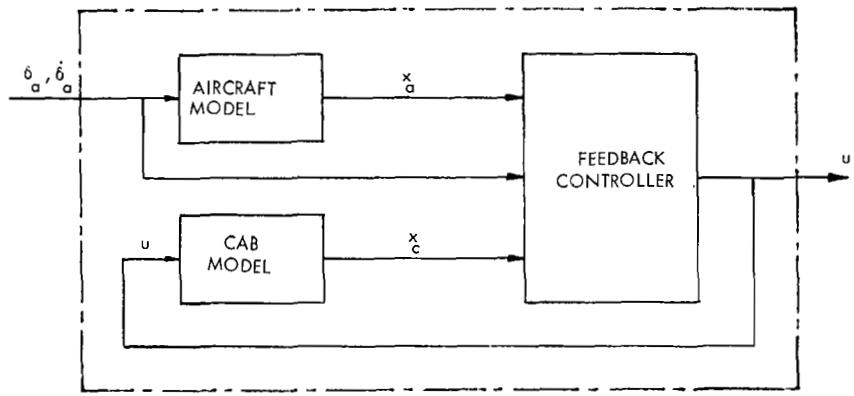

(b) vector form

Fig. 4-17 (con't)

$$A_1 = -g_a - N_{56}/q_{\ddot{\theta}}$$

$$A_2 = -f_a - N_{55}/q_{\dot{\theta}}$$

$$A_3 = -e_a - N_{54}/q_{\theta}$$

$$A_4 = -N_{53}/q_{\ddot{\theta}}$$

$$A_5 = d_a - N_{52}/q_{\dot{\theta}}$$

$$A_6 = -\frac{c_a N_{53} + N_{56}}{k q_{\ddot{\theta}} + \sqrt{q_{\dot{\theta}}\, q_{\ddot{\theta}}}}$$

$$A_7 = 2\xi_2\omega_2 - \sqrt{q_{\dot{\theta}}/q_{\ddot{\theta}}}$$

$$A_8 = \omega_2^2$$

$$B_1 = -N_{36}/q_{\ddot{y}}$$

$$B_2 = b_a - N_{35}/q_{\ddot{y}}$$

$$B_3 = -N_{34}/q_{\ddot{y}}$$

$$B_4 = -a_a - N_{33}/q_{\ddot{y}}$$

$$B_5 = -N_{32}/q_{\ddot{y}}$$

$$B_6 = c_a - \frac{c_a(N_{33} + \sqrt{q_{\dot{y}}\, q_{\ddot{y}}}) + N_{36}}{k q_{\ddot{y}} + \sqrt{q_{\dot{y}}\, q_{\ddot{y}}}}$$

$$B_7 = 2\xi_1\omega_1 - \sqrt{q_{\dot{y}}/q_{\ddot{y}}}$$

$$B_8 = \omega_1^2$$

$$F_1 = -\frac{k_2(k_1 + k_3)}{k_1^2 k_3^2}$$

$$F_2 = \frac{k_2}{k_1 k_3}$$

$$F_3 = -\frac{k_2}{k_1^2(k_1 - k_3)}$$

$$F_4 = \frac{k_2}{k_3^2(k_1 - k_3)}$$

4.4 Summary and Discussion of Simulation Results

The results achieved in the simulation studies described above demonstrate the capability of the quasi-optimum control technique to maintain the cab within the allowable motion limits. The nature of the motion within these limits, however, can have virtually limitless variety, depending on the parameters selected.

For purposes of comparison the motion time-histories for the single trapezoidal pulse input with different washout schemes (Figures 4-4, 4-7, 4-12, 4-15) are reproduced side-by-side in Fig. 4-18 (a - d). Also shown as Fig. 4-18e is the set of time histories obtained by the use of the conventional high-pass filter technique described in Section 1.

The differences between use of jerk weighting and no use thereof can be seen by comparison of Fig. 4-18a with Fig. 4-18c and Fig. 4-18b with Fig. 4-18d. The cases with jerk weighting demonstrate good phase fidelity at the expense of highly attenuated magnitudes of cab acceleration and jerk, and vice-versa for the cases without jerk weighting.

On the other hand, the differences that result from using a linear washout ($\beta = 1$) and a nonlinear washout ($\beta > 1$) can be seen by comparing Fig. 4-18a with Fig. 4-18b and Fig. 4-18c with Fig. 4-18d. The nonlinear washout in general provides a better phase and "onset" (i.e. high rates of change) relationships with somewhat distorted magnitude relation.

Fig. 4-18e shows the translational trajectories resulting from a control system using a conventional frequency-domain design technique in which the cab is driven by a position servo whose command signal is in turn generated by a high-pass filter with aircraft acceleration as an input. The cab motion in this scheme is governed by the second-order system

$$\ddot{y}_c + 2\xi\omega\dot{y}_c + \omega^2 y_c = \ddot{y}_a \tag{4.67}$$

where ξ and ω are constant parameters and the aircraft acceleration $\ddot{y}_a$ is taken directly from the aircraft dynamics. Adjustment of the damping ξ results in varied magnitude relations and the adjustment of the cut-off frequency ω results in varied phase relations. For $\xi = 0.7$ and $\omega = 1.0$, the high-pass filter provides the limited cab excursion as shown in Fig. 4-18e. The one particular feature of this washout scheme is that the cab is returned to

the starting position at the end of transient. The price paid for this advantage is the spurious overshoots in the acceleation and jerk time-histories and a fairly low fidelity of phase relationships.

A comment concerning realization is in order. Since a digital computer was employed in performing these simulations, and the objective was to establish the capability of the technique, no effort was made to simplify the control laws obtained by these techniques. If a large-scale digital computer were used to control the physical simulator there probably would be no need to simplify the resulting expressions. If the control laws were to be realized by means of a digital computer of limited capability or by means of an analog computer, however, it would be highly desirable to simplify the results. Examination of each of the terms in the expressions for the control laws ought to reveal that some are negligible with respect to the others, and can be omitted without sacrificing performance. By this means it would appear possible to achieve control laws which can be implemented by small-scale digital or analog computers.

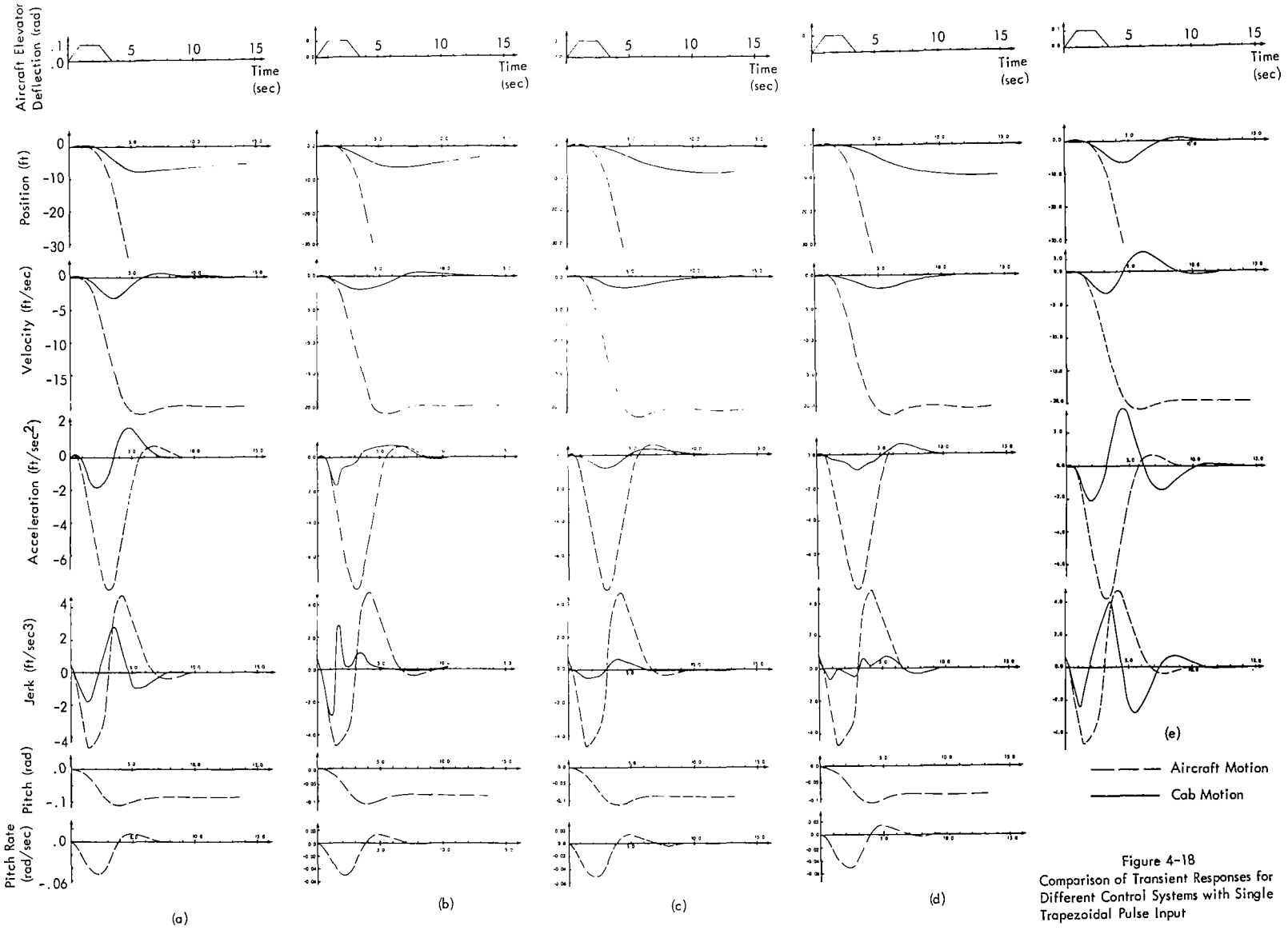

Figure 4-18
Comparison of Transient Responses for Different Control Systems with Single Trapezoidal Pulse Input

4.5 Comparison with Conventional "Washout" Circuits

Although considerations of modern control theory were dominant in the development of the control laws described above, the resulting controls are not entirely different from those obtained by conventional washout techniques. In the latter, the washout circuit it interposed between the aircraft ("command") acceleration and the acceleration input to the cab drive system. It is assumed that the servo for the cab is capable of producing a cab motion for which the acceleration is identical to the output of the washout circuit. Consequently, the comparison between the control laws developed in this study and conventional washout schemes can be made by means of the differential equations relating the cab acceleration (with the quasi-optimum control law in use) to the aircraft acceleration and ppssibly other variables.

The forms of the "quasi-optimum filter" for the (M_1, L_2) case can be derived by first substituting the numerical data in Table 4.2 into (4.36) to yield

$$\begin{aligned} C_1 &= y_c - 10\dot{y}_c + 35\dot{\delta}_a \\ C_2 &= -10\dot{y}_c + 32.32\dot{\delta}_a \\ C_3 &= -1.708\dot{\delta}_a \end{aligned} \tag{4.68}$$

Substitution of (4.68) into (4.37) and subsequently into the closed-loop system equation (4.29) results in the linear $(M_1, L_2)_{\beta=1}$ "filter" equation

$$\begin{aligned} \dddot{y}_c + 2.3\,\ddot{y}_c + 0.072\,\dot{y}_c &= \ddot{y}_a + 7.547\,\dot{\delta}_a \\ \ddot{\theta}_c &= \ddot{\theta}_a \end{aligned} \tag{4.69}$$

Since these equations are linear, (4.69) can be expressed by means of transfer functions. For the vertical channel

$$\ddot{Y}_c(s) = \frac{s^2}{s^2 + 2.3s + 0.072}\left[\ddot{Y}_a(s) + 7.547\,\Delta_a(s)\right]$$

where $\ddot{Y}_c(s)$, $\ddot{Y}_a(s)$, and $\Delta_a(s)$ are the Laplace transforms of $\ddot{y}_c$, $\ddot{y}_a$, and $\dot{\delta}_a$, respectively.

The block diagram equivalent of this relation is given in Fig. 4-19. This control law can be interpreted as a high-pass filter (with a natural frequency ω of 0.268 rad/sec and a damping factor ξ of 4.29) operating on the sum of the aircraft acceleration and a constant times the aircraft elevator deflection. The principal difference between the filter of Fig. 4-19 and the conventional washout circuit is the additional direct input signal from the elevator deflection. It would thus appear that the flexibility of this additional input permits one to achieve somewhat superior performance.

It is noted that no washout is employed for pitch motion because it is not needed for maintaining the pitch angle between physical limits.

To obtain the nonlinear $(M_1, L_2)_{\beta=2}$ "filter" equation, it is noted from (4.68) and (4.38) that terms including C_3 can be dropped without significant effect. Thus from (4.68), (4.38) and (4.29) we have

$$\ddot{y}_c = \ddot{y}_a + 0.0002\,(0.08\,C_1^3 - 8.97\,C_2^3 + 4.9438\,C_1C_2^2 - 1.0067\,C_1^2C_2) \qquad (4.70)$$

$$\ddot{\theta}_c = \ddot{\theta}_a$$

with C_1, C_2, C_3 given by (4.68). Owing to the nonlinearities in (4.70), this system cannot be represented by means of transfers. It can be realized, however, through the use of nonlinear analog devices (multipliers). The block diagram of the realization is given in Fig. 4-20

For the linear $(M_2, L_2)_{\beta=1}$ case, the quasi-optimum fliter is obtained by using the data in Table 4-2 to (4.46), (4.51), (4.63), (4.64), and (4.65),

$$\begin{aligned}
\sqrt{q_{\ddot{y}}/q_{\dddot{y}}} &= 0.014 \\
N_{32}/q_{\dddot{y}} &= 0.0044 \\
N_{33}/q_{\dddot{y}} &= 0.0065 \\
N_{34}/q_{\dddot{y}} &= -1.0225 \\
N_{35}/q_{\dddot{y}} &= 0.0184 \\
N_{36}/q_{\dddot{y}} &= -0.8976 \\
q_3/q_{\dddot{y}} &= -0.00075
\end{aligned} \qquad (4.71)$$

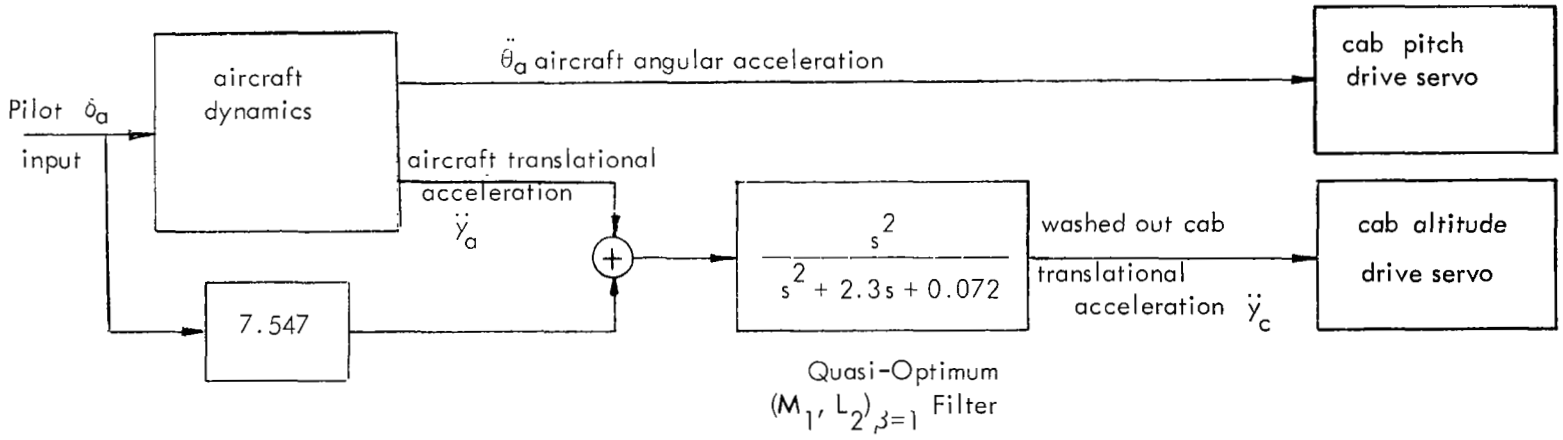

Fig. 4.19

Linear Quasi-Optimum Wash-Out Block Diagram

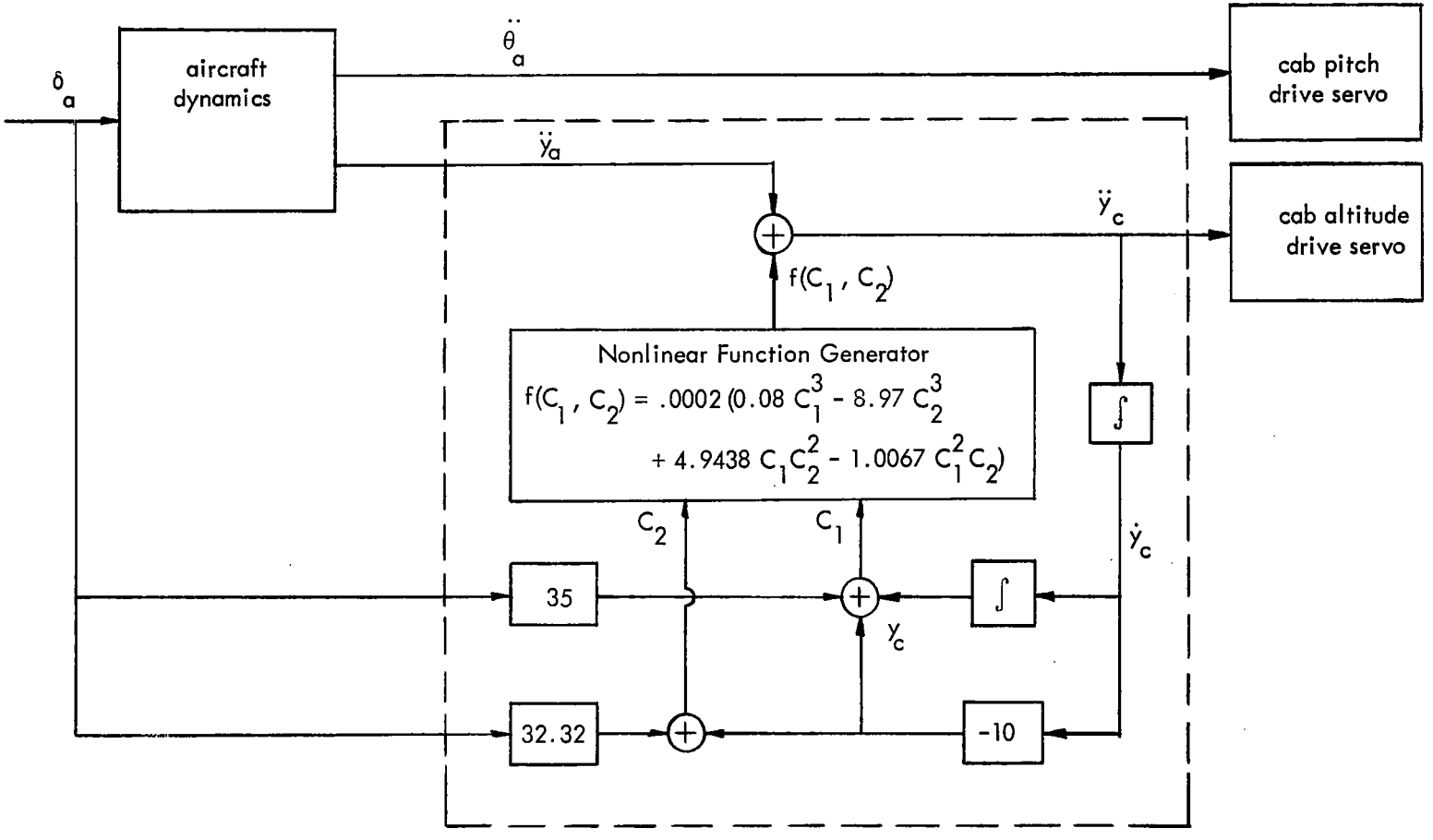

Quasi-Optimum

$(M_1, L_2)_{\beta=2}$ Filter

Fig. 4-20

Nonlinear Quasi-Optimum Wash-Out Block Diagram

$$
\begin{aligned}
C_1 &= y_c - 100\,\ddot{y}_c - 367.5\,\dddot{y}_a \\
C_2 &= \dot{y}_c + 10\,\ddot{y}_c + 35\,\dddot{y}_a \\
C_3 &= 100\,\ddot{y}_c + 368.4\,\dddot{y}_a \\
C_4 &= -0.92\,\dddot{y}_a \\
D_1 &= -121152.0 \\
D_2 &= -8896833.0 \\
D_3 &= -874.4 \\
D_4 &= -0.1241
\end{aligned}
\tag{4.72}
$$

$$
\rho_3 = -6.058\,y_c - 444.8\,\dot{y}_c - 3847.0\,\ddot{y}_c - 13359.4\,\dddot{y}_a \tag{4.73}
$$

Substitution of (4.71), (4.72) and (4.73) into the closed-loop system equation (4.59) results in the "filter" equation

$$
\begin{aligned}
\dddot{y}_c + 0.2308\,\ddot{y}_c + 0.0267\,\dot{y}_c + 0.00036\,y_c \\
= 0.2\ \dddot{y}_a - 0.0065\,\ddot{y}_a - 0.0044\,\dot{y}_a - 0.0184\,\dot{\theta}_a \\
+ 1.0225\,\theta_a + 0.00075\dot{\delta}_a + 0.8976\delta_a \\
\ddot{\theta}_c = \ddot{\theta}_a
\end{aligned}
\tag{4.74}
$$

Fig. 4-21 shows the block diagram for mechanizing the system (4.74).

The approximate nonlinear $(M_2, L_2)_{\beta=1.25}$ "filter" equation is obtained by substituting (4.66) into (4.59),

$$
\begin{aligned}
\dddot{y}_c + 0.0112\,\ddot{y}_c = \dddot{y}_a - 0.142\,(\ddot{y}_a)^{1.5} - 0.0048\,\ddot{y}_a - 0.0033\,\dot{y}_a \\
- 0.0108\,\dot{\theta}_a + 0.7579\,\theta_a + 0.6659\,\delta_a + 0.2052\,\dot{\delta}_a \\
\ddot{\theta}_c = \ddot{\theta}_a
\end{aligned}
\tag{4.75}
$$

Although it would not be practical to express the nonlinear "filter" equation (4.75) in block diagrams such as shown in Fig. 4-21, their mechanization by means of either digital computer or analog computer presents no particular difficulties.

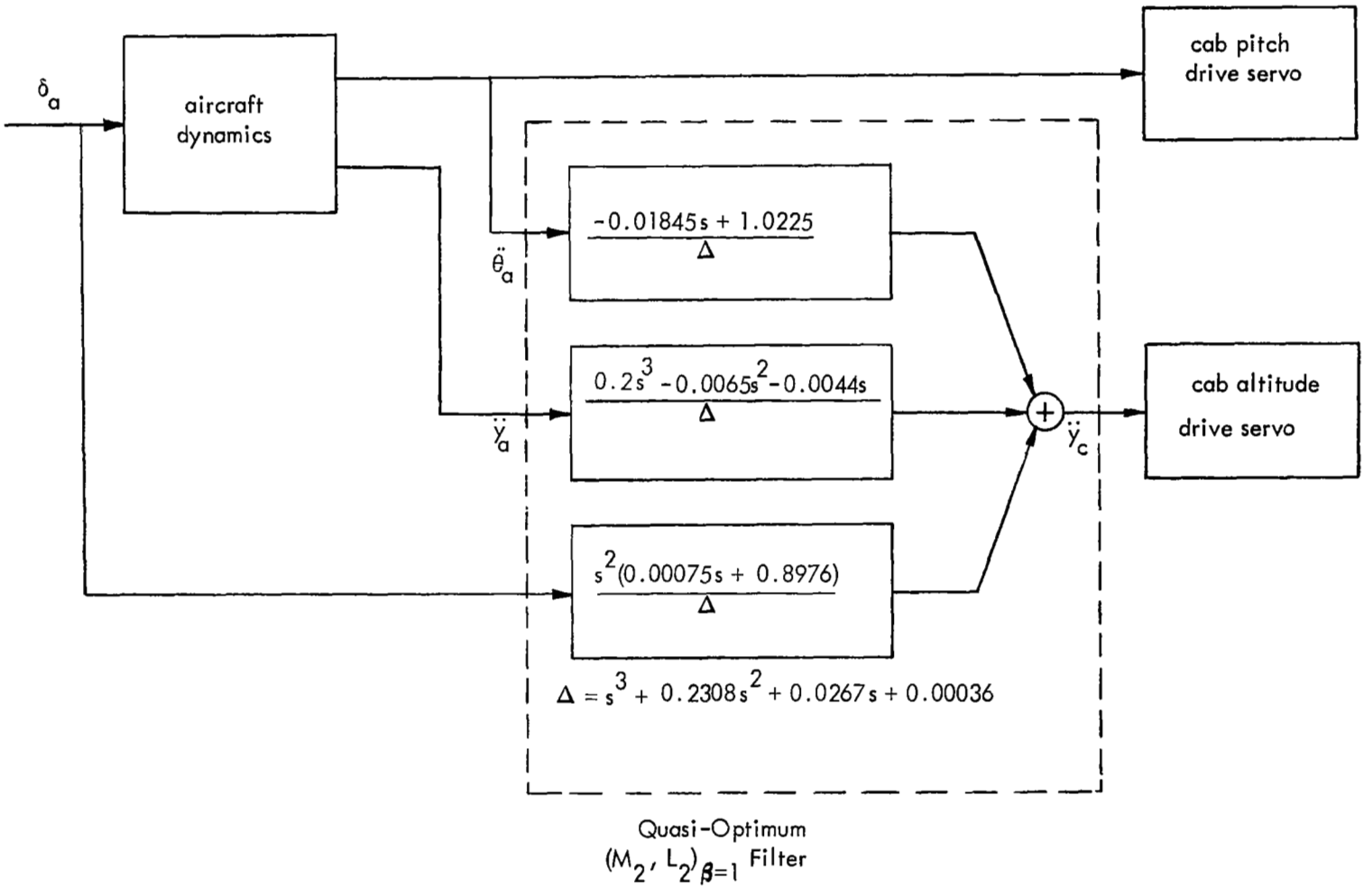

Fig. 4-21

Linear Quasi-Optimum Wash-Out Block Diagram

5. CONCLUSIONS AND RECOMMENDATIONS

The results of this investigation demonstrate that the quasi-optimum control technique is potentially applicable to the design of motion simulators with limited motion capability. In particular, it was shown that in the restricted case of two degrees-of-freedom, it is possible to maintain the cab within limits of ± 10 ft. and achieve acceleration time histories which may be preferable to those achieved by use of conventional washout techniques.

The landing maneuver exemplifies the problem with which all control techniques must contend. In this case the aircraft vertical velocity starts at zero and goes to a non-zero value, i.e. the integral of the acceleration is non-zero. The cab, however, must ultimately reach a velocity of zero and hence the integral of its acceleration must be zero. Hence the control law for the cab must approximate a physical quantity with a non-zero integral by another quantity whose integral is zero. This limitation is inherent in all techniques. The real question thus devolves from the definition of the approximation criterion. It is demonstrated, we believe, that the quasi-optimum control technique is capable of achieving the desired approximation once it is defined.

It is generally agreed that the approximation should maintain reasonable fidelity of amplitude, phase, and onset of acceleration. Since the improvement in fidelity of one of these factors generally reduces the fidelity of one or both of the others, however, it would be desirable to have a quantitative measure of the relative importance of these.

Two methods of shedding light on this difficult problem are feasible. The first method would be to experimentally appraise the importance of these factors by performing simulations with control schemes designed to emphasize specific factors. The quasi-optimum control technique described can be efficiently used to "tailor" the control law to the feature to be emphasized. In particular, the control laws described in Section 4 would seem to be good candidates for initial experiments.

The second method would employ a model of the human vestibular system and neural processing. Such a model would take into account the experimentally determined

dynamic characteristics and such nonlinear phenomena as threshold and latency time. The performance criterion would be based on the difference between the output of the model sensing the aircraft acceleration and the model sensing the cab acceleration, rather than upon acceleration errors and the derivatives thereof.

It is recommended that both approaches be pursued in subsequent studies, as it is expected that their results will be complementary.

As a possible preliminary to the experimental and analytical studies, just described, it might be desirable to pursue the studies described in Section 4 to greater depth by considering a larger variety of test inputs and a larger variety of penalty functions $L(x_c)$ in combination with the two quadratic weighting matrices.

Since the technique considered was restricted to the case of two degrees-of-freedom it must be extended to the more general six degree-of-freedom case before it can be employed in a realistic application. It is believed that the extension to six degrees-of-freedom will introduce few technical difficulties and recommend that the extension be performed.

In summary, our conclusions are

- The quasi-optimum control technique is potentially of considerable value in the design of control systems for moving-base simulators.

- Additional effort is required in establishing performance criteria and in extending the analysis to six degrees-of-freedom.

In view of the latter conclusion, the following additional effort is recommended:

- More exhaustive study of the two degree-of-freedom case.

- Experimental assessment of control laws for two degree-of-freedom case by means of actual flight simulation at the Ames Research Center.

- Analytical development of performance criterion through use of model of kinesthetic sensor and data processing.

- Extension of analysis and simulation to general case of six degrees-of-freedom.

REFERENCES

1. Friedland, B., Thau, F.E., Cohen, V.D., and Ellis, J., "Study of Quasi-Optimum Feedback Control Techniques", NASA CR-527, August 1966.

2. Friedland, B., Thau, F.E., Welt, S., Ling, C.K. and Schilder, M., "Additional Studies of Quasi-Optimum Feedback Control Techniques", NASA CR-1099, July 1968.

NASA-Langley, 1970 —— 11